Multi-criteria decision analysis for groundwater potential zones delineation using geospatial tools and Analytical Hierarchy Process (AHP) in Nand Samand Catchment, Rajasthan, India

Dimple[1] · Pradeep Kumar Singh[1] · Mahesh Kothari[1] · Kamal Kishore Yadav[2] ·
Sita Ram Bhakar[1]

Abstract

Developing groundwater potential zones (GWPz) is important to determine the realistic groundwater availability scenario and to formulate plans for its optimal utilization to achieve groundwater sustainability. This investigation aimed to delineate GWPz in the Nand Samand Catchment, Rajasthan, India, utilizing an integrated method of remote sensing, geographic information system, and analytical hierarchy process (AHP). The present study used ten thematic layers, viz., lineament density, well recharge, geomorphology, soil, topographic elevation, slope, rainfall, transmissivity, the post-monsoon water level in the well and land use/land cover for the GWPz delineation. The delineated GWPz in the research area were classified as 'good (G),' 'moderate (M),' 'poor (P)' and 'very poor (VP).' Results showed that 'good' GWPz constituted about 21.23% of the catchment area. The southeast area and small patches of the western side of the research area have 'moderate' groundwater potential, covering 53.18% of the total area. Approximately 23.77% area was found with poor GWPz. In the research area, 1.82% area represents very poor groundwater potential. In the present study, the GWPz map was validated using sixteen randomly selected wells yield data (liters per day), and an accuracy of 81.25% was found with the delineated GWPz map. Furthermore, the receiver operating characteristics curve was also used for the validation, indicating a satisfactory accuracy prediction (AUC = 0.889). Validation by both methods justifies the efficiency of the AHP technique for the groundwater potential zoning. Finally, this work establishes a viable method for assessing the potential availability of groundwater, which will be helpful in the future for the planning and managing groundwater resources.

Keywords AHP · GWPz · Geographic information system · Thematic layers · Nand Samand Catchment · Rajasthan

✉ Dimple
   dimpibachchan20@gmail.com

Extended author information available on the last page of the article

1 Introduction

Groundwater (subsurface water) plays a vital environmental role in continuous river flows, societies, and the ecosphere globally. Additionally, it is a immense source of fresh water on the planet (UNESCO, 2018). In arid and semi-arid areas, subsurface water is the prime available water resource for many purposes, including domestic and irrigation (Dimple et al., 2022). Of the freshwater available on the earth, nearly 30% is present in subsurface water, and < 1% is present in lakes and rivers. The CGWB (2017) report states that the total yearly groundwater recharge is 432 Billion Cubic Meters (BCM), and the yearly exploitable groundwater resources are 393 BCM. The yearly extraction of groundwater for all applications is 249 BCM, of which 221 BCM (89%) is used for agriculture and 25 BCM (10%) for domestic needs (CGWB, 2017). Recent studies have reported that approximately 20% of globally groundwater is used for the purposes of irrigation (Adimalla & Venkatayogi, 2018; Saeid et al., 2018). Almost 2 billion people depend on groundwater for drinking water (Abe & Ersado, 2022). Because it has a greater potential for availability and is less likely to become contaminated than surface water, groundwater is an important source of water supplies in all climatic regions. This includes both urban and rural areas of both developed and developing nations. This is because climatic conditions threaten the reliability of surface water. Groundwater is an ever-changing resource influenced by various factors, including geomorphology, lithology, topography, slope, precipitation, soil, drainage pattern, LULC, and hydrological conditions (Acharya, 2017; Murmu et al., 2019; Singh et al., 2011). Several regions of the country's water level have dropped quickly during the last two decades (Jasrotia et al., 2016).

Traditional groundwater research techniques, such as drilling, geophysical, geological, and hydro-geological approaches, are expensive and time-consuming, necessitating the deployment of large human and financial resources. Groundwater potential mapping (GPM) is a cost-effective method for identifying spatial differences in groundwater recharge potential with fewer sources (Arabameri et al., 2019), whereas nowadays RS and GIS are important tools that may be used to predict groundwater resources at a minimal cost quickly and can be used efficiently for groundwater research before resorting to more extensive and costly surveying procedures (Priya et al., 2022). Groundwater potential zone development is typically influenced by a variety of factors, including denudation, structural characteristics, terrain, drainage, climate, and the type, thickness and structural makeup of the underlying rocks. The effect of these factors on groundwater recharge varies by location. Linear structures such as fractures and faults, for example, can operate as conduits or barriers for groundwater movement. As a result, they are powerful variables in determining potential recharge zones. Groundwater recharging often favors buffer zones of 300–500 m near the lineament (Ahmed et al., 2021). However, these aspects must be considered to outline and identify an area's groundwater recharge potential (GWRP).

Presently, groundwater is decreased at a rate of 800 km^3 per year globally. Irrigated agricultural lands are a significant source of groundwater depletion (Burek et al., 2016). Due to a lack of surface water, water scarcity in arid and semi-arid areas has considerably grown (Castillo et al., 2022). According to studies, groundwater resources offer more than 70% of the water supply (Sahu et al., 2022; Suliman et al., 2022) and are overexploited, with a rate of depletion of 545 km^3/year (Makonyo & Msabi, 2021). The estimated annual groundwater usage is almost 230 km^3, and India is a largest user of groundwater globally (World

Bank, 2010). In addition, more than 60% of the groundwater is used for irrigation, and 85% is used for domestic supplies. Due to this, groundwater levels have declined by more than 4 m in different parts of the country (CGWB, 2014). Groundwater used for irrigation is approximately 245×10^9 m^3 in India (CGWB, 2014). Groundwater productivity potential in semi-arid hard rock aquifers remains restrained by shallow, fractured, and weathered formations (Machiwal & Jha, 2014). Because of the consequences of climate change and population increase, among other variables, which impose severe stress on accessible surface water sources in these locations, groundwater supplies provide the majority of household, agricultural and industrial water demands in these hard rock terrains (Edmunds et al., 2003). Shallow hard rock aquifers account for roughly 73% (2.386 million km^2) of India's total land area (Machiwal & Singh, 2015).

Nowadays, the integration of RS and GIS techniques is practiced as a faster, more precise and more cost-efficient way to identify the many factors relevant to the groundwater potential zones (GWPz) (Fagbohun, 2018; Lentswe & Molwalefhe, 2020; Vishwakarma et al., 2021). Additionally, RS and GIS technology development has supported the delineation of groundwater potential zones in vast regions quickly. These methods have become very useful and cost-effective through high-resolution satellite images, mostly in inaccessible locations. Many researchers have reported many studies on using geographic information systems in groundwater management and monitoring, like delineation of GWPz (Bera et al., 2020; Bhattacharya et al., 2020; Das et al., 2017; Kumar et al., 2016; Machiwal & Singh, 2015; Pande et al., 2019; Rajasekhar et al., 2020). Most of these studies have relied on integrating the relative weights of various thematic layers, such as geology, geomorphology, lineament density, drainage density, post-monsoon water table depth, relative slope position (RSP), topographic wetness index (TWI), slope, etc., within a GIS environment (Ahmed et al., 2021; Akbari et al., 2021; Yeh et al., 2009). Many multi-criteria decision analysis (MCDA) models are used by researchers for groundwater potential zoning like multi-influencing factors (MIF) (Ahmed et al., 2021), full consistency method, best–worst method (Akbari et al., 2021), analytical networking process (ANP) (Mir et al., 2021; Singha et al., 2019), fuzzy analytic hierarchy process (Chaudhry et al., 2019; Jesiya & Gopinath, 2020; Singh et al., 2021; Sresto et al., 2021), weight of evidence (WoE) and frequency ratio (FR) (Rane & Jayaraj, 2021); the AHP (Castillo et al., 2022) technique has the potential to determine groundwater prospect zones (Arulbalaji et al., 2019). Delineation of GWPz through proper modeling techniques is important to mitigate the water scarcity problem in the semi-arid region (Bera et al., 2020). No such studies have been done in the NSC regarding the delineation of GWPz mapping due to a lack of knowledge about the aquifer parameters, factors which influence the groundwater and integrated approach of RS, GIS, AHP, etc. Because agriculture is the primary occupation in this area, a precise groundwater potential map for this catchment is firmly needed. There is a need to map the aquifers to know the quantum and quality of groundwater resources. Therefore, the present work aimed to identify the GWPz in the NSC, using GIS and AHP techniques for managing and planning groundwater resources. Geospatial technology is a novel concept that integrates RS, GIS, and AHP, and it has proved to be an effective tool for delineating GWPz. AHP was introduced by (Saaty, 1980) to solve complex decision-making through pairwise comparisons. AHP is a helpful method for prospecting GWPZs (Sahu et al., 2022; Sajil-Kumar et al., 2022). Shekhar and Pandey (2015) reported that utilizing AHP in combination with GIS is a time-saving and effective

way of managing spatial data. Various researchers have exercised AHP to identify the groundwater potential zones by calculating the weights of various TLs and their respective classes (Machiwal et al., 2011; Manap et al., 2014; Rahmati et al., 2015; Singh et al., 2018). The literature suggests that GIS and AHP techniques could be utilized for groundwater potential zoning studies. The study's novelty was the evaluation of field datasets by combining multi-criteria decision problems to delineate GWPz in the catchment. Therefore, the current study utilized geospatial tools and the AHP method to identify groundwater potential sites in the Nand Samand Catchment to improve groundwater resource utilization. Understanding this valuable water resource is critical to ensuring its long-term development and management. The research may contribute to creating, planning, and managing sustainable groundwater resources.

1.1 Study area

Nand Samand Dam is located in Rajsamand district of Rajasthan state, India, between 24°0′0.5″ and 26°0′0.5″ N and 72°59′59.50″ and 73°59′59.50″ E coordinates. The location map is shown in Fig. 1. The research area comes under an arid to semi-arid climate with an annual average rainfall (2001–2011) of 640.45 mm (CGWB, 2013). The district's central and eastern areas are largely flat, forming the foothill of the Aravalli ranges. The general slope of the terrain is toward the east. The main river of the district is Banas, with its tributaries, i.e., Khari and Chandrabhaga generating an excellent drainage system in the area (GWDR, 2013). The total study area is 865.18 km^2, with a maximum elevation (1318 m) and the minimum elevation (570 m) above mean sea level.
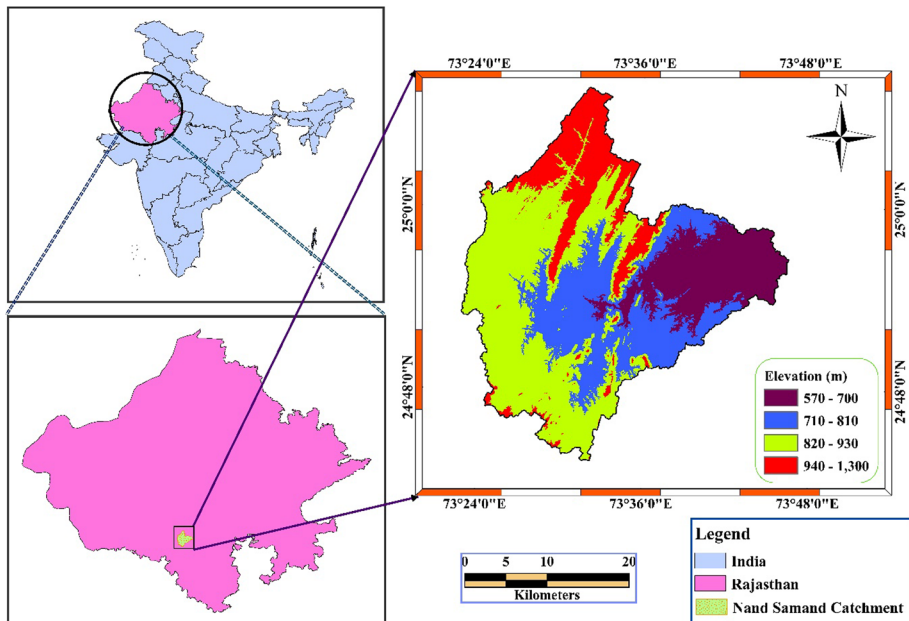

Fig. 1 Nand Samand Catchment

2 Materials and methods

In this study, we have used primary and secondary data for mapping the GWPz of the study area. After reviewing published literature, ten criteria for geospatial mapping of groundwater potential zones were chosen for the current study. Thematic layers like well recharge, geomorphology, lineament density, slope, topographic elevation, transmissivity, post-monsoon water level, soil, rainfall and LULC were created using RS and conventional/existing data in Arc-GIS 10.1 environment. Data description is summarized in Table 1. The current study created a digital elevation model (DEM) of the research area using Advanced Spaceborne Thermal Emission and Reflection Radiometer (ASTER) elevation data (30 m spatial resolution). The research area's base map was created using SOI (Survey of India) topographic sheets (45G-12, 45H-5, 6, 9, 10, 13, 45NG-9) of 1:50,000 scale. These SOI topographic maps were georeferenced in ArcGIS 10.1 using the World Geodetic System (WGS) 84 datum and the Universal Transverse Mercator (UTM) zone 43N projection. Soil data of the study area were collected from the National Bureau of Soil Survey (NBSS) and Land Use Planning (LUP), Udaipur, Rajasthan. The unsupervised classification was used to extract the LULC categories within the catchment. Digitally processed raw satellite images included geometric correction, image enlargement, image interpretation and multispectral categorization. Additionally, unsupervised image classification was used to categorize land use types. Satellite data were analyzed using visual interpretation techniques to identify and describe various objects associated with urban areas. After detailed analysis, the result was compared and corrected by data collected from different locations of the area. The methodology developed is given in Fig. 2. The Landsat image was used to map the lineament density, and the DEM was used to generate the hillshade map. Figure 3 depicts the study's methodological flowchart.

2.1 AHP weight assignment and normalization

The MCDA methodology for delineating the Nand Samand Catchment GWPz was produced by integrating various GIS tools and the AHP method. The most significant aspect of the integrated analysis is the weight assigned to all classes. As a result, it is highly dependent on the assignment of suitable weight (Murmu et al., 2019). The current research employed the AHP approach, which Saaty (1980) introduced. The benefit of hierarchy is that it enables us to focus our judgment independently on each of the numerous attributes required to make solid decisions (Saaty, 1990). The relative importance values for all thematic layers and their associated characteristics were calculated using a standard Saaty's 1–9 scale, where '1' indicates "Equal Importance (EI)" for two themes and '9' indicates "extreme importance" for one theme relative to the other TLs, as presented in Table 2.

The following procedure was exercised to calculate the final weights assigned to each theme layer (Murmu et al., 2019):

(1) Using Eq. (1), add the data in the individual column of the pairwise matrix (PWM) (Table 3).

$$L_j = \sum_{i,j=1}^{n} C_{ij} \tag{1}$$

where $L_j =$ the pairwise matrix's total data in each column and $C_{ij} =$ at the ith row and jth column, the number assigned to each condition.

Table 1 Data collected to identify GWPz in this work are detailed

| S. no.	Data type	Specification	Scale/resolution	Duration	Reference
1	Geodetic toposheet		1:50,000		
2	Soil map	Soil texture	1:250,000		NBSS and LUP, Regional Research Station, Udaipur
3	Aquifer parameters	Transmissivity and specific yield data at 10 sites		December, 2020	Pumping tests were undertaken, and data analysis was performed
4	Groundwater levels	95 site data	4 seasons of 2 years	Pre-monsoon season (2019 and 2020), post-monsoon season (2019 and 2020)	Solinst, Canada, TLC (temperature level conductivity) meter was used to measure the water level of the well
5	Digital elevation model, slope and lineament density	Raster (ASTER DEM)	30 m (spatial resolution)		USGS website (https://earthexplorer.usgs.gov)
6	Rainfall data		1 km^2 (spatial resolution)	2011–2020	(https://crudata.uea.ac.uk/cru/data/hrg/)
7	Geomorphology		1:50,000		Geology survey of India (https://bhukosh.gsi.gov.in/Bhukosh/Public)
8	Satellite imagery LULC	Landsat 8 OLI	30 m resolution		https://earthexplorer.usgs.gov
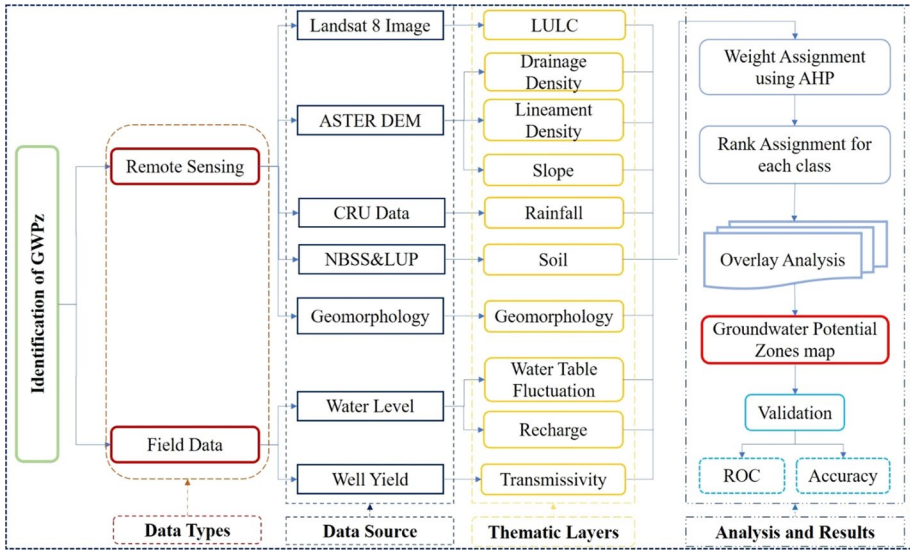
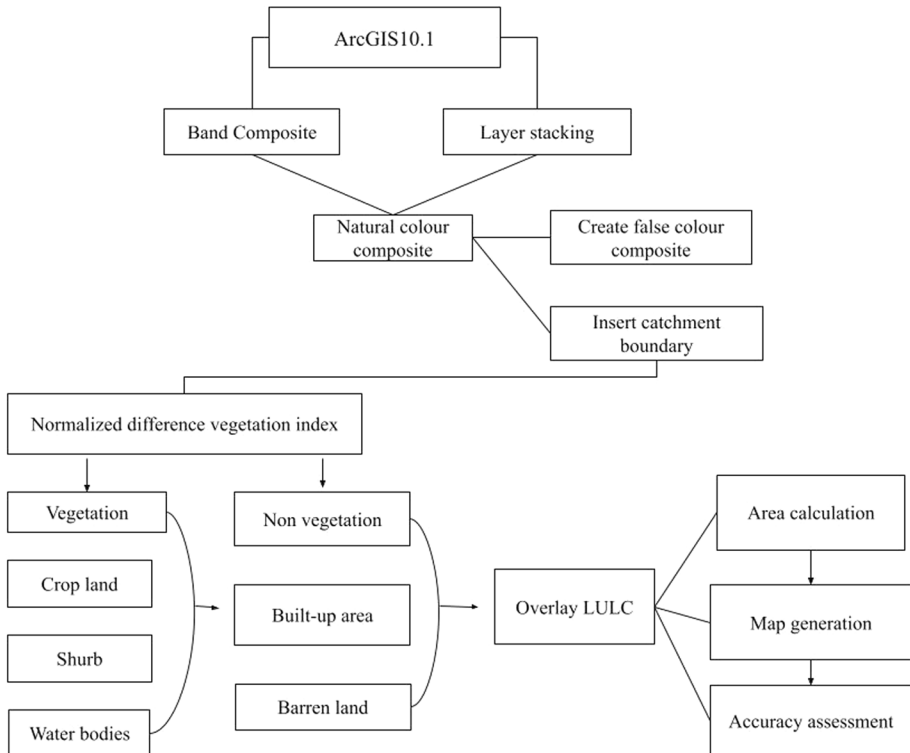**Fig. 2** Methodology flow diagram of the present study

Fig. 3 Unsupervised classification of Landsat image

Table 2 Saaty's scale (26)

Importance number	Definitions
1	EI
2	E-M
3	M
4	M-S
5	S
6	S-V
7	V-S
8	V-E
9	Ex

EI equal importance, *E-M* equal to moderate importance, *M* moderate importance, *M-S* moderate to strong importance, *S* strong importance, *S-V* strong to very strong importance, *V-S* very strong importance, *V-E* very to extremely strong importance, *Ex* extreme importance

Table 3 Pairwise comparison matrix of ten thematic layers

	T	Ld	WD	TE	S	Sl	RE	LU	RF	GM
T	1	2	3	3.5	4	4.5	5	5.5	6	7
L_d	0.5	1	2	3	3.5	4	4.5	5	5.5	6
WD	0.333333	0.5	1	2	3	3.5	4	4.5	5	5.5
TE	0.285714	0.333333	0.5	1	2	3	3.5	4	4.5	5
S	0.25	0.285714	0.333333	0.5	1	2	3	3.5	4	4.5
Sl	0.222222	0.25	0.285714	0.333333	0.5	1	2	3	3.5	4
RE	0.2	0.222222	0.25	0.285714	0.333333	0.5	1	2	3	3.5
LU	0.181818	0.2	0.222222	0.25	0.285714	0.333333	0.5	1	2	3
RF	0.166667	0.181818	0.2	0.222222	0.25	0.285714	0.333333	0.5	1	2
GM	0.142857	0.166667	0.181818	0.2	0.222222	0.25	0.285714	0.333333	0.5	1

T transmissivity, *Ld* lineament density, *WD* post-monsoon groundwater depth, *TE* topographic elevation, *S* soil, *Sl* slope, *RE* recharge, *LU* land use/land cover, *RF* rainfall, *GM* geomorphology

(2) To construct a normalized PWM, divide each element in the matrix by the sum of its columns (Table 4)

$$X_{ij} = \frac{C_{ij}}{L_j}$$

(2)

where X_{ij} = the value that appears in the ith row and jth column of the normalized PWM.

Table 4 Normalized pairwise matrix and weight of each thematic layer

	T	L_d	WD	TE	Soil	Slope	RE	LU	RF	GM	Normalized weight
T	0.30	0.39	0.38	0.31	0.27	0.23	0.21	0.19	0.17	0.17	0.26
L_d	0.15	0.19	0.25	0.27	0.23	0.21	0.19	0.17	0.16	0.14	0.20
WD	0.10	0.10	0.13	0.18	0.20	0.18	0.17	0.15	0.14	0.13	0.15
TE	0.09	0.06	0.06	0.09	0.13	0.15	0.15	0.14	0.13	0.12	0.11
Soil	0.08	0.06	0.04	0.04	0.07	0.10	0.12	0.12	0.11	0.11	0.09
Slope	0.07	0.05	0.04	0.03	0.03	0.05	0.08	0.10	0.10	0.10	0.06
RE	0.06	0.04	0.03	0.03	0.02	0.03	0.04	0.07	0.09	0.08	0.05
LU	0.06	0.04	0.03	0.02	0.02	0.02	0.02	0.03	0.06	0.07	0.04
RF	0.05	0.04	0.03	0.02	0.02	0.01	0.01	0.02	0.03	0.05	0.03
GM	0.04	0.03	0.02	0.02	0.01	0.01	0.01	0.01	0.01	0.02	0.02

(3) Using the following equation, divide the sum of the normalized row of the matrix by the number of criteria used to calculate standard weights (*N*) to obtain the normalized row of the matrix.

$$W_i = \frac{\sum X_{ij}}{N} \tag{3}$$

where W_i = standard weight.

2.2 Consistency analysis

Multiply the consistency vector by the pairwise comparison matrix values of theme layers (Murmu et al., 2019).

(4) Principal eigenvalue (λ_{max}) computed by the following formula

$$\lambda_{max} = \sum \left(C_{ij} X_{ij} \right) \tag{4}$$

(5) The consistency ratio (CR) was computed as (Saaty, 1980):

$$C_{ratio} = \frac{C_{index}}{C_{random}} \tag{5}$$

where C_{random} = random consistency index (RI), the values of which were acquired from Saaty's standard table (1980).

Table 5 Random inconsistency values	n	I	II	III	IV	V	VI	VII	VIII	IX	IX
	RI	0	0	0.58	0.9	1.12	1.24	1.32	1.41	1.45	1.49

(6) The following formula was used to calculate the consistency index (CI):

$$C_{index} = \frac{\lambda_{max} - 1}{n - 1} \tag{6}$$

where n = number of thematic variables.

If the CR value is ≤ 0.1, the inconsistency is permissible; otherwise, the subjective assessment must be revised (Saaty, 1990). Table 5 shows the RI values for n criterion (Murmu et al., 2019).

2.3 Determination of groundwater potential zones

The groundwater potential index (GWPI) is a dimensionless number that aids in defining areas with high groundwater potential (Kumar & Krishna, 2018). The total weights of various polygons in the integrated layer were calculated using the following equation.

$$GWPI = \left(\begin{array}{l} GM_w GM_{wi} + S_w S_{wi} + SL_w SL_{wi} + TE_w TE_{wi} + LU_w LU_{wi} + \\ WD_w WD_{wi} + RE_w RE_{wi} + TR_w TR_{wi} + RF_w RF_{wi} + Ld_w Ld_{wi} \end{array} \right)$$

where GM denotes the geomorphology, S for soil type, SL for slope, TE for topographic elevation, LU for land use, WD for post-monsoon groundwater depth, RE for groundwater recharge, TR for transmissivity, RF for rainfall, Ld for lineament density, w for the normalized weight of a theme and wi for the normalized weight of the individual features of a theme.

2.4 Validation of groundwater potential zones

Before explaining a model, whether stochastic or deterministic, it must first be validated. The model's scientific significance is determined by its validation (Al-Manmi et al., 2021). Eventually, to assess the accuracy of the proposed technique, the existing wells location map in the study has been used. Sixteen-well yield data resulting from the pumping test have been used. To verify the accuracy of the current work in various groundwater potential zones, the well yield points were superimposed on the final groundwater potential zones map. Many studies have used a similar validation method (Ahmed et al., 2021; Akbari et al., 2021; Al-Manmi et al., 2021; Arulbalaji et al., 2019; Priya et al., 2022; Trabelsi et al., 2022). Also, the ROC method (Castillo et al., 2022; Jhariya et al., 2021; Kaewdum & Chotpantarat, 2021; Melese & Belay, 2022; Pandey et al., 2022) was used for the validation of the AHP technique.

3 Results and discussion

3.1 Hydrologic TLs

Groundwater occurrence and movement are influenced by many factors, including geological structure, topography, slope, rainfall, soil, soil porosity, drainage density and pattern, LULC, and hydrological conditions of the area, as well as the interdependence of these parameters (Murmu et al., 2019). Groundwater in the hard rocks (consolidated) occurs under water table conditions in the zone of weathering and fracturing, joints, fissures and bedding planes; correct identification of the GWPz is important to prevent economic loss, wasting time and effort. In the present study, ten thematic layers were identified as the influencing factors, such as recharge, geomorphology, lineament density, slope, topographic elevation, transmissivity, post-monsoon water level, soil, rainfall and LULC to delineate the GWPz. The number of thematic layers selection depends on the data available in a given area. Each theme layer has specific information about the occurrence of groundwater. The groundwater prospect map was created by merging ten themed maps into GIS environment, utilizing remote sensing and conventional data. Out of these thematic maps, ASTER data were used to generate topographic elevation, lineament density and slope maps, whereas conventional data were used to generate soil map. Thematic maps were prepared in the ArcGIS environment to understand baseline information of different groundwater-related parameters. Each factor evaluating the GWPz in the study area is classified into four classes. These thematic maps were converted to raster data sets with the same pixel size (resolution), and different weightage was assigned using the AHP method. Each map was reclassified based on the weight values generated.

3.1.1 Geomorphology

The geomorphology of an area consists of many landforms and structural elements that are important in determining groundwater potential and prospects because they influence groundwater movement. In the present study, analog-type districts maps were extracted from the Geology survey of India (https://bhukosh.gsi.gov.in/Bhukosh/Public) and clipped the selected study area geomorphology in the ArcGIS software to generate a thematic layer. The geomorphological features of the research area can be divided into four categories, which are as follows: (i) waterbodies, (ii) alluvial plain, (iii) denudational hills and valleys, and (iv) structural hills (Fig. 4). Waterbodies encompassing an area of 16.49 km^2 (1.91% of the total area), alluvial plain encompassing an area of 14.35 km^2 (1.66% of the total area), denudational hills and valleys encompassing an area of 460.01 km^2 (53.17% of the total area), and structural hills encompassing an area of 374.32 km^2 (43.27% of the total area). Denudational hills and valleys dominate the study area. Denudational origins are characterized by gently sloping plains covered in weathered material conducive to groundwater recharge (Murmu et al., 2019). Authors have used geomorphology as one of the most influencing factors in the GWPz (Anand et al., 2021; Arulbalaji et al., 2019). The maximum weight is given for valley fill, water bodies, coastal plain of fluvial origin and minimum weight assigned to lower lateritic plateau and denudational hills (Arulbalaji et al., 2019).

Table 6 shows the final geomorphological feature weights. The weights allocated to all the thematic layers and the AHP procedure were used to derive the normalized weights as given in Tables 3 and 4. Consistency analysis calculation:

$$1 * 0.30 + 2 * 0.15 + 3 * 0.10 + 3.5 * 0.09 + 4 * 0.08$$
$$+ 4.5 * 0.07 + 5 * 0.06 + 5.5 * 0.06 + 6 * 0.05 + 7 * 0.04 = 3.05.$$
$$0.5 * 0.39 + 1 * 0.19 + 2 * 0.10 + 3 * 0.06 + 3.5 * 0.06$$
$$+ 4 * 0.05 + 4.5 * 0.04 + 5 * 0.04 + 5.5 * 0.04 + 6 * 0.03 = 1.95.$$
$$0.33 * 0.38 + 0.5 * 0.25 + 1 * 0.13 + 2 * 0.06$$
$$+ 3 * 0.04 + 3.5 * 0.04 + 4 * 0.03 + 4.5 * 0.03 + 5 * 0.03 + 5.5 * 0.02 = 1.25.$$
$$0.29 * 0.31 + 0.33 * 0.27 + 0.5 * 0.18 + 1 * 0.09 + 2 * 0.04$$
$$+ 3 * 0.03 + 3.5 * 0.03 + 4 * 0.02 + 4.5 * 0.02 + 5 * 0.02 = 0.89.$$
$$0.25 * 0.27 + 0.29 * 0.23 + 0.33 * 0.20 + 0.5 * 0.13 + 1 * 0.07$$
$$+ 2 * 0.03 + 3 * 0.02 + 3.5 * 0.02 + 4 * 0.02 + 4.5 + 0.01 = 0.66.$$
$$0.22 * 0.23 + 0.25 * 0.21 + 0.29 * 0.18 + 0.33 * 0.15 + 0.50 * 0.10$$
$$+ 1 * 0.05 + 2 * 0.03 + 3 * 0.02 + 3.5 * 0.01 + 4 * 0.01 = 0.52.$$
$$0.20 * 0.21 + 0.22 * 0.19 + 0.25 * 0.17 + 0.29 * 0.15 + 0.33 * 0.12$$
$$+ 0.50 * 0.08 + 1 * 0.04 + 2 * 0.02 + 3 * 0.01 + 3.5 * 0.01 = 0.41.$$
$$0.18 * 0.19 + 0.20 * 0.17 + 0.22 * 0.15 + 0.25 * 0.14 + 0.29 * 0.12$$
$$+ 0.33 * 0.10 + 0.50 * 0.07 + 1 * 0.03 + 2 * 0.02 + 3 * 0.01 = 0.34.$$
$$0.17 * 0.17 + 0.18 * 0.16 + 0.20 * 0.14 + 0.22 * 0.13 + 0.25 * 0.11$$
$$+ 0.29 * 0.10 + 0.33 * 0.09 + 0.50 * 0.06 + 1 * 0.03 + 2 * 0.01 = 0.29.$$
$$0.14 * 0.17 + 0.17 * 0.14 + 0.18 * 0.13 + 0.20 * 0.12 + 0.22 * 0.11$$
$$+ 0.25 * 0.10 + 0.29 * 0.08 + 0.33 * 0.07 + 0.50 * 0.05 + 1 * 0.02 = 0.24.$$

The consistency vector (λ_{max}) value is determined as 9.59. From Eqs. (5) and (6), consistency ratio was determined as (-0.03) and found acceptable.

3.1.2 Slope

The slope significantly defines groundwater's presence and recharge situations in a particular region (Bagyaraj et al., 2013). Slope gradient directly impacts rainfall infiltration and is thus an indicator of appropriateness for groundwater prospecting. Because of the high surface run-off, the steeper the slope, the lesser will be recharge, allowing inadequate time for the water to infiltrate through the surface and replenish the saturated zone (Ghosh et al., 2016).

The slope of the study area was classified into five categories as very low (0–3%), low (3–8%), moderate (8–15%), high (15–30%) and very high (>30%) presented in Fig. 5. The highest weight is assigned for flat and gentle slopes, and the lowest weight is assigned for the steep and very steep slope. Arulbalaji et al. (2019) also similarly assigned the weight to the slope layer. The majority of the research area falls in the 3–8 percent slope class (35.16% of the total area). As a result, the maximum portion of the study area has a sloping slope which is favorable for water retention. Using a scale of 1–9, the ratings were assigned
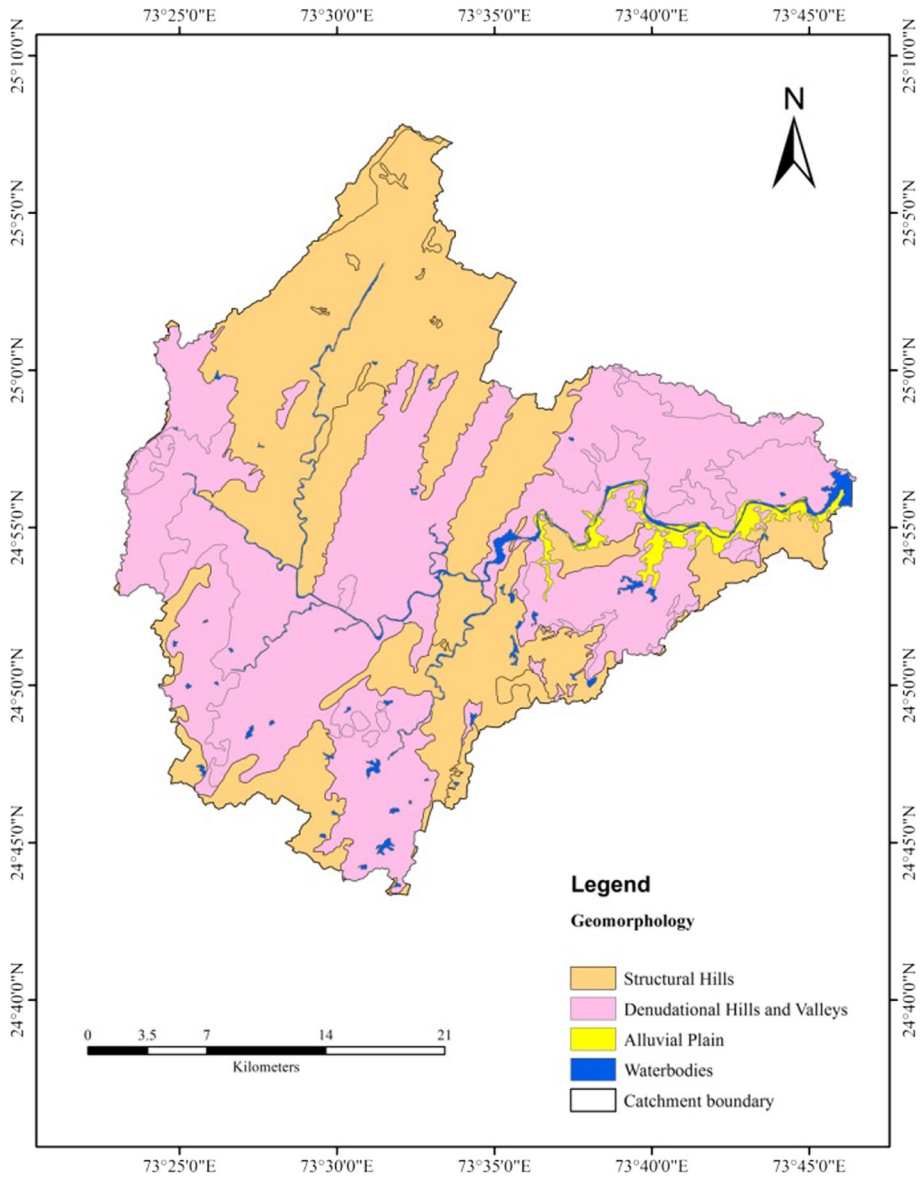
Fig. 4 Thematic layer of geomorphology

Table 6 Normalized weights of all thematic layer classes for groundwater potential zoning

Factor	Groundwater class	Weight allocated	Normalized weight
Geomorphology			
Waterbodies	VG	8	0.381
Alluvial plain	G	7	0.333
Denudational hills and valleys	Poor	5	0.238
Structural hills	Very poor	1	0.048
Slope (%)			
<3	VG	8	0.400
3–8	G	6	0.300
8–15	M	4	0.200
15–30	Poor	1	0.050
>30	Very poor	1	0.050
Lineament density (km/km^2)			
0–32	Low	1	0.077
0.32–0.64	Moderate	3	0.231
0.64–0.96	High	4	0.308
0.96–1.28	Very high	5	0.385
Transmissivity classes (m^2/day)			
105–136	Extremely poor	1	0.074
136–167	Very poor	1.5	0.111
167–198	Very poor	1.5	0.111
198–229	Poor	2	0.148
229–260	Poor	2	0.148
260–291	Moderate	2.5	0.185
291–322	Good	3	0.222
Recharge classes (cm/year)			
<10	Poor	2	0.091
10–15	Moderate	3	0.136
15–20	Moderate	4	0.182
20–30	Good	6	0.273
>30	Very good	7	0.318
Post-monsoon groundwater depth (m bgs)			
<4	VG	8.5	0.405
4–8	G	7.5	0.357
8–12	M	5	0.238
Drainage density (km/km^2)			
0–0.3	Very low	5	0.333
0.3–0.6	Low	4	0.267
0.6–1.0	Moderate	3	0.200
1.0–1.5	High	2	0.133
1.5–2.82	Very high	1	0.067
Rainfall map (mm)			
585.43–603.86	Very low	4	0.133
603.86–615.70	Low	5	0.167
615.70–625.97	Moderate	6	0.200
625.970–636.50	High	7	0.233

Table 6 (continued)

Factor	Groundwater class	Weight allocated	Normal-ized weight
636.50–652.56	Very high	8	0.267
Topographic elevation (m)			
570–690	VG	8	0.348
690–794	G	7	0.304
794–890	M	5	0.217
890–1000	Poor	2	0.087
1000–1318	Very poor	1	0.043
LULC			
Waterbodies	Good	6	0.293
Cropland	Good	5.5	0.268
Built-up area	Very poor	2	0.098
Barren land	Poor	3	0.146
Shrub	Moderate	4	0.195
Soil			
Loamy skeletal	Very good	8	0.364
Coarse loamy	G	7	0.318
Fine loamy	M	6	0.273
Rock outcrops	Poor	1	0.045

VG very good, *G* good, *M* moderate

to distinct slope classes. Higher ranks were given to slope classes with a smaller percentage of slopes due to the flat terrain's ability to retain more groundwater, while lower ranks were assigned to steeper slopes with more run-off and less infiltration (Kumar & Krishna, 2018; Nag & Ghosh, 2013). Table 6 shows the final weights for the slope classes.

3.1.3 Soil

The capacity of a soil to hold and transmit soil moisture in profile depends on its texture, porosity and soil structure. For example, heavy soils provide effective capillary tubes for moisture movement due to their fine texture and porosity. Due to large particles and pores, with minimum fine capillary pores, there is minor soil moisture movement in loose sandy soils. Soil texture has a significant impact on groundwater recharging and surface run-off. The soil type, infiltration rate, percolation and permeability of the soil affect groundwater recharge (Jasrotia et al., 2016). The soil map of the study area was collected from the NBSS and LUP, at 1:250,000 scale. ArcGIS software was used to scan and digitize the soil map. The research area comprises four soil types: loamy skeletal, coarse loamy, fine loamy and rocks outcrops. It is seen from Fig. 6 that most of the research area is dominated by fine loamy to rock outcrops soil which is about 91.48% of the total research area. Loamy/loamy skeletal soils have a high positive association with groundwater recharge, having maximum weightage values, signifying maximum groundwater recharge potential (Bera et al., 2020; Doke et al., 2021), while rock outcrops soils were negatively associated with groundwater
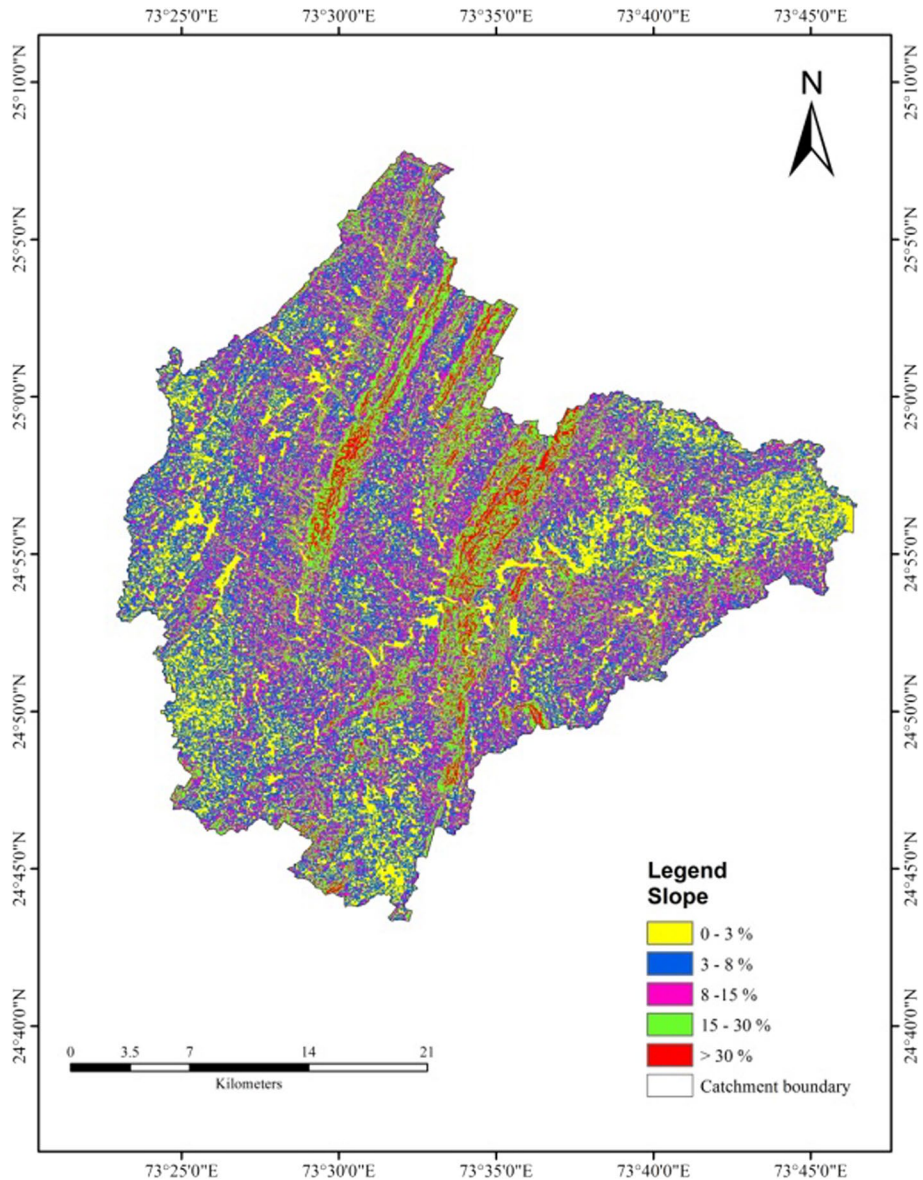
Fig. 5 Slope map

recharge; therefore, the lesser score is assigned. Table 6 shows the final weights for the soil classes.

3.1.4 Topographic elevation

The DEM of the present research area was generated using Advanced Spaceborne Thermal Emission and Reflection Radiometer-30 m (ASTER) data (Source: https://earthexplo

rer.usgs.gov). The topographic data are available in the GeoTIFF raster file format with a pixel resolution of 30 m. The topography file was imported to ArcGIS, and DEM was created. The most effective recharge site would be lower than the river's level, allowing the water to be easily diverted by gravity. Given that topography (land surface height) is one of the factors affecting groundwater potential, the present study included a topographical elevation map as one of the TLs. The higher is elevation, the lesser is groundwater available. Figure 7 depicts the topographic map. The study area has been classified into five topographic elevation classes based on its topographic elevation: (i) 570–690 m, (ii) 690–794 m, (iii) 794–890 m, (iv) 890–1000 m and (v) 1000–1318 m. Northern areas of the research area have the highest topographic elevations, which results in the most run-off and hence reduced potential of rainwater infiltration. The study area is dominated by topographic elevations 794–890 m in 316.42 km^2 areas, which is about 36.57% of the total area.

3.1.5 Land Use/Land Cover (LULC)

According to Shaban et al. (2006), plant cover promotes groundwater recharge in various ways, containing biological decomposition of the plants roots, which offers a conduit for water to percolate onto the surface by loosening the rock and soil. Also, the plants act as barrier and retards the surface run-off velocity, which gives more infiltration opportunity time to the running water and thus more groundwater recharge. A LULC thematic layer was distinguished into five different classes: (i) waterbodies, (ii) cropland, (iii) built-up area, (iv) barren land and (v) shrub as shown in Fig. 8. Different LULC cover classes were ranked according to their importance in groundwater recharge potential. The LULC classes, like forest and agricultural land, hold substantially more water than the built-up land, barren land and rocky surfaces (Arulbalaji et al., 2019). Crop areas were given a higher rating than other land uses since they require more irrigation water, which results in groundwater recharge. Because of the shallow soil, the surface run-off rate is higher on barren ground. Hence, it receives a lower score. Because the built-up terrain is concrete, the surface run-off is high, and the infiltration rate is low. As a result, built-up land is assigned the lowest score (Doke et al., 2021).

3.1.6 Post-monsoon groundwater depth (WD)

The WD in the research area ranges from 0.27 m Below Ground Surface (bgs) to 9.2 m bgs. Groundwater at maximum depths was assigned a higher weight. Figure 9 depicts WD map of the research area, revealing that the groundwater depth < 4 m bgs in 91.54%, 4–8 m bgs in 8.33% and 8–12 m bgs in 0.13% of the total research area. The deeper groundwater levels in the study area's north, east parts, and the small and scattered patches are a result of excessive groundwater pumping for irrigation. Figure 9 shows that less variance occurs during the post-monsoon season because the underlying hard rock aquifer system has a low specific yield, allowing water levels to rise fast in response to rainy-season recharge (Machiwal et al., 2017).
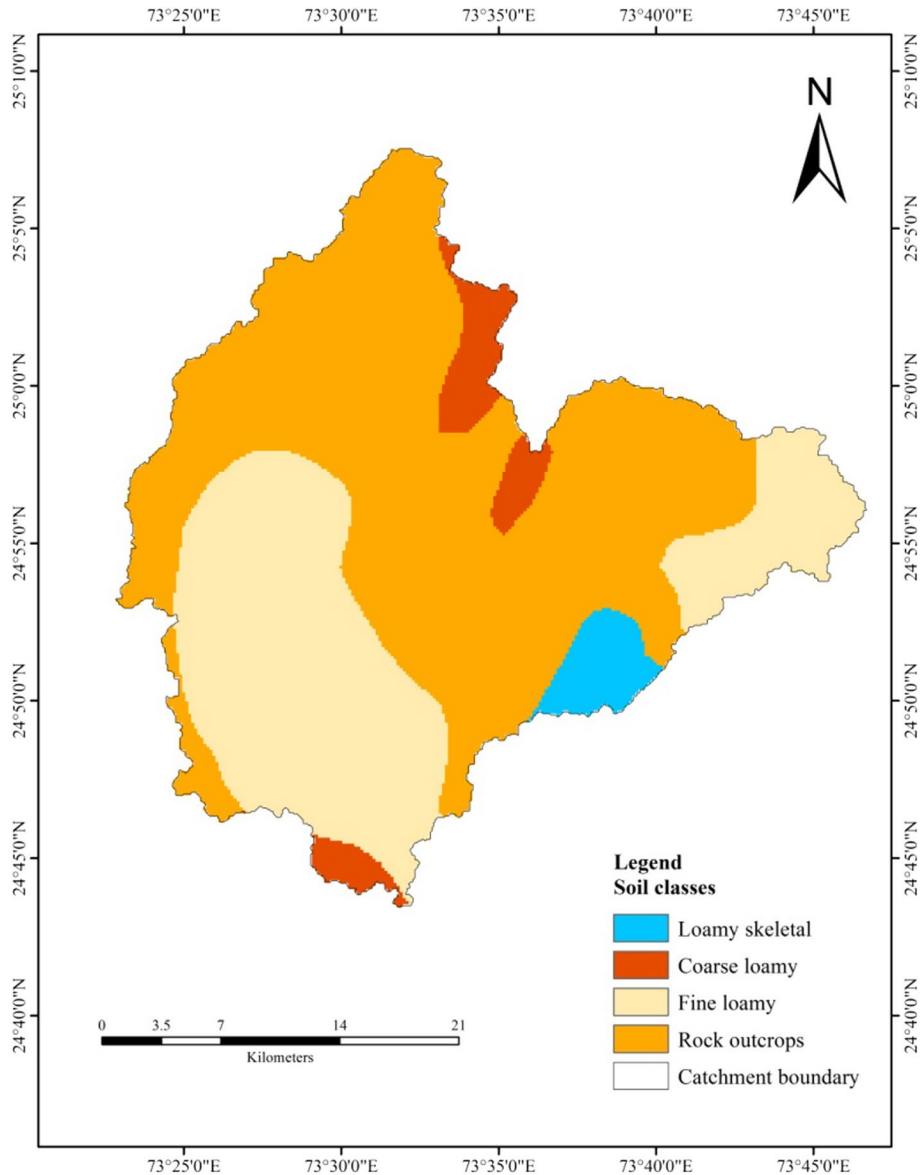
Fig. 6 Thematic layer of soil

3.1.7 Recharge

The study area's annual net groundwater recharge varies between 0.27 and 42.27 cm. The recharge map was created using the Inverse Distance Weighted Moving Average (IDWMA) technique with point recharge values (95 locations). The recharge area has been divided into five recharging zones based on these recharge estimates: (i) < 10 cm/year (yr), (ii) 10–15 cm/yr, (iii) 15–20 cm/yr (iv) 20–30 cm/yr and (v) > 30 cm/yr as seen from Fig. 10.
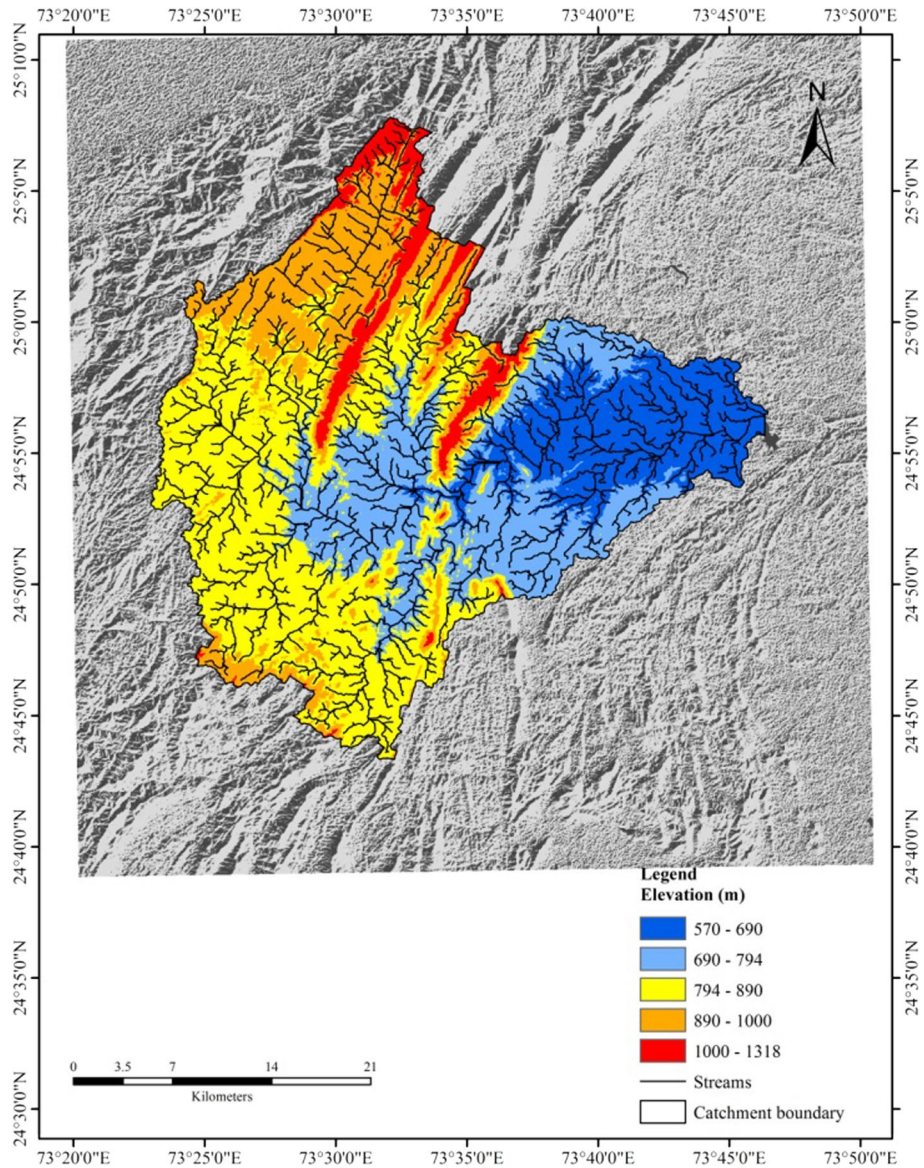
Fig. 7 Topographic elevation map

Figure 10 indicates that a net recharge rate of < 10 cm/year is predominant in the research area, covering approximately 50.05% of the study area. Net recharging at a rate of between 10 and 15 cm/year corresponds to approximately 25.32% of the study area. The northeast part of the research area has a maximum recharge rate (> 30 cm/yr). Increased rainfall in any given area equates to increased recharge possibilities (Machiwal et al., 2011, 2017; Murmu et al., 2019).
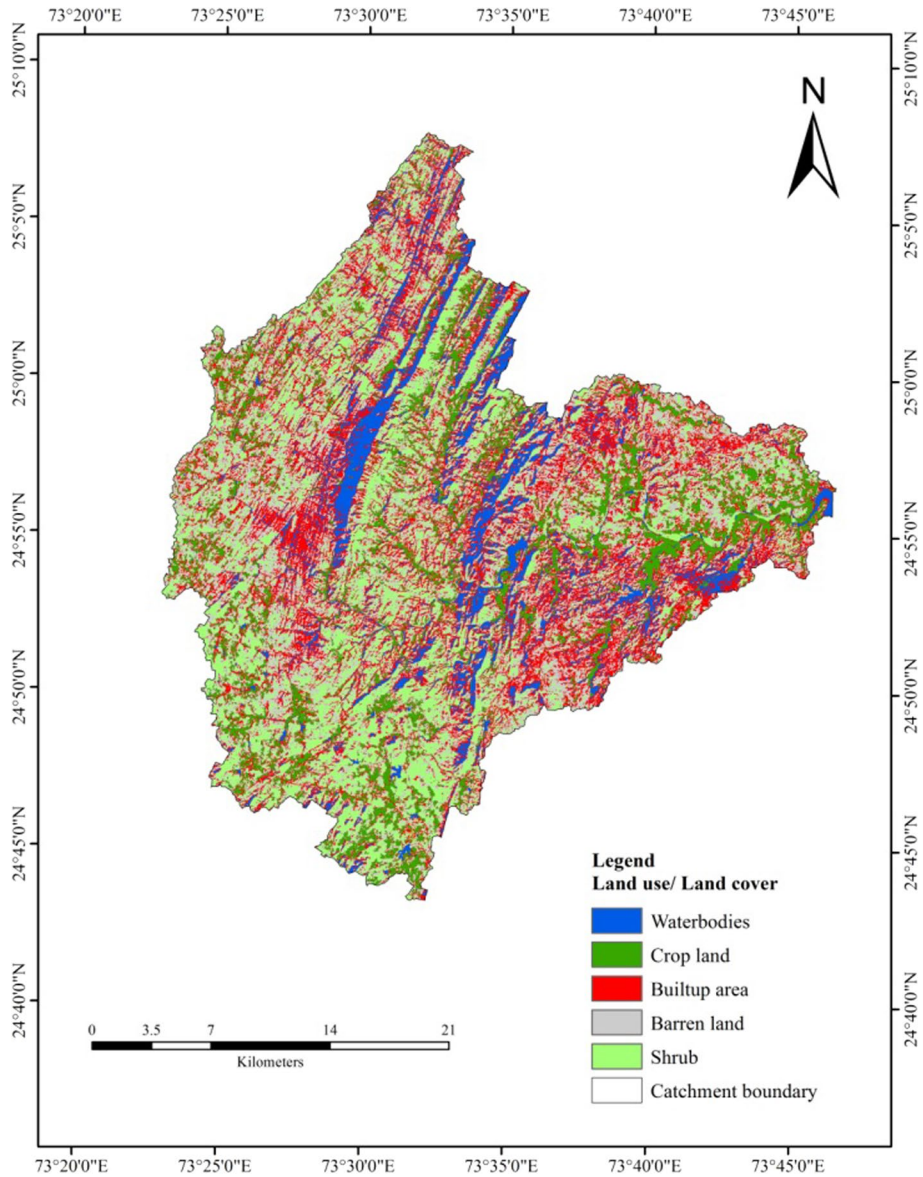
Fig. 8 LULC map

3.1.8 Transmissivity

Transmissivity data were generated by conducting pumping test in the study area and were used to generate a point map of transmissivity. A transmissivity raster map was created after interpolating this point map using the interpolation technique, viz. Inverse Distance
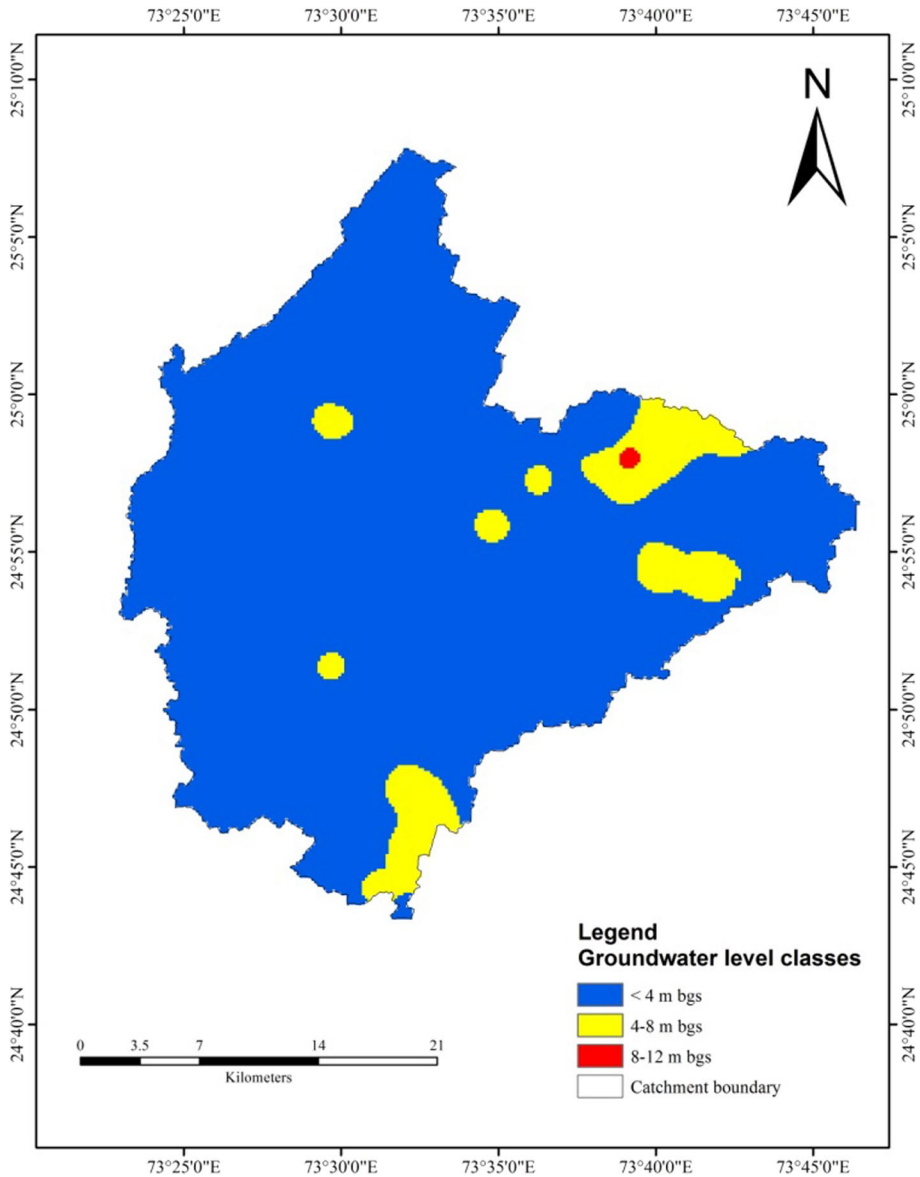
Fig. 9 Post-monsoon groundwater depth map

Weighting (IDW) technique in the ArcGIS environment. It is found that the transmissivity in the present study area ranges from 105.10 to 321.90 m^2/day. The area was classified into seven transmissivity classes based on these values, namely extremely poor (105–136 m^2/day), very poor (136–167 m^2/day), very poor (167–198 m^2/day), poor (198–229 m^2/day), poor (229–260 m^2/day), moderate (260–291 m^2/day) and good (291–322 m^2/day) as given in Fig. 11. The transmissivity map shows that a low transmissivity (105–136 m^2/day) is confined to small patches in the Northwest parts of the research
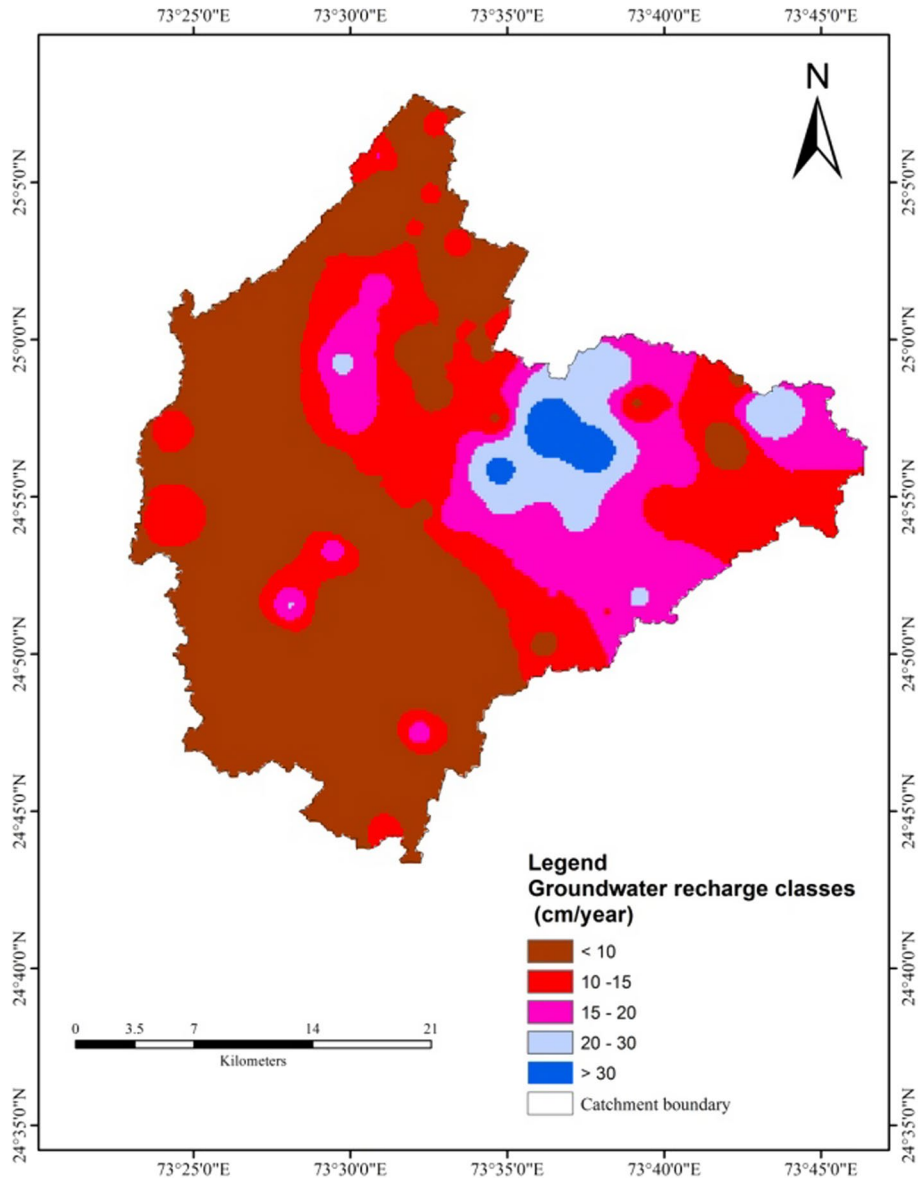
Fig. 10 Recharge map

area. The dominance of transmissivity from 167 to 198 m^2/day is maximum, which is about 32.19% of the total research area. Anand et al. (2021) used transmissivity as one of the thematic layers in the Bhavani River basin; the transmissivity of the ranges from 48.14 to 455.42 m^2/day.

3.1.9 Rainfall

Rainfall makes a significant contribution to groundwater recharge. In arid areas, rainfall is considered as one of the most influential factors in groundwater recharge capability (Ahmed et al., 2019). More rainfall in any given location provides more chances of recharge (Machiwal et al., 2011). In this study, 10-years (2011–2020) rainfall data were taken (https://crudata.uea.ac.uk/cru/data/hrg/) to make a rainfall map of the research area (Fig. 12; Table 6). The spatial distribution map of rainfall was prepared using IDW interpolation method. The average annual rainfall in the research area is divided into five categories, i.e., very low (585.43–603.86 mm), low (603.86–615.70 mm), moderate (615.70–625.97 mm), high (625.970–636.50 mm) and very high (636.50–652.56 mm). The maximum intensity of rainfall (636.50–652.56 mm) was found in the southern most part of the catchment area. Maximum intensity rainfall regions have a high weightage value, which covers approximately 134.21 km^2 (15.51%) area, signifying excellent groundwater potential (Bera et al., 2020). Rain with a high intensity and a short duration results in less infiltration and more surface run-off; rain with a low intensity and a long duration causes more infiltration than run-off (Arulbalaji et al., 2019).

3.1.10 Lineament density (Ld)

Lineament characteristics like joints, cracks, and faults are particularly important hydrogeologically because they operate like a conduit for groundwater occurrence, resulting in greater porosity, and so serving as a GWPz (Mukherjee et al., 2012). Lineaments have the potential to play an important role in GWPz by maximizing soil infiltration capacity and ease to groundwater flow and movement (Das & Pardeshi, 2018). Lineament density and drainage density are inversely proportional to each other. Good GWPz are available where lineament density is maximum and drainage density is minimum with gentle slope (Ahmed et al., 2021; Arulbalaji et al., 2019). The research area's lineament orientation is primarily along the North East–South West and North West–South East directions, as seen by a "rose diagram" (Fig. 13). As reported by Harinarayana et al. (2000), the normalized transmissivity around the lineaments is maximum, and there is a strong correlation between increased fracture density and higher well yields. As a result, locations with maximum Ld have a greater effect on GWPz. The Ld of the catchment ranges from 0 to 1.28 km/km^2 (Fig. 14) and the Ld was regrouped into four classes, viz., very high (0.96–1.28 km/km^2), high (0.64–0.96 km/km^2), moderate (0.32–0.64 km/km^2) and low (0–0.32 km/km^2). Groundwater development has a significant potential in areas with extremely high to high lineament density (Bera et al., 2020). Table 6 contains the final weights for the Ld.

3.2 Delineation of GWPz

A better understanding of groundwater potential is important for planning and long-term sustainable development. This information is vital for designing and implementing corrective measures to improve groundwater recharge processes. The parameters considered here are lineament density, well recharge, geomorphology, soil, topographic elevation, slope, rainfall, transmissivity, the post-monsoon water level in the well and land use/land cover (LULC). Groundwater potential zones in the Nand Samand Catchment have been generated using the weighted overlay approach in ArcGIS environment. The resulting map is divided into 'good (G),' 'moderate (M),' 'poor (P)' and 'very poor (VP)' GWPz. Following the
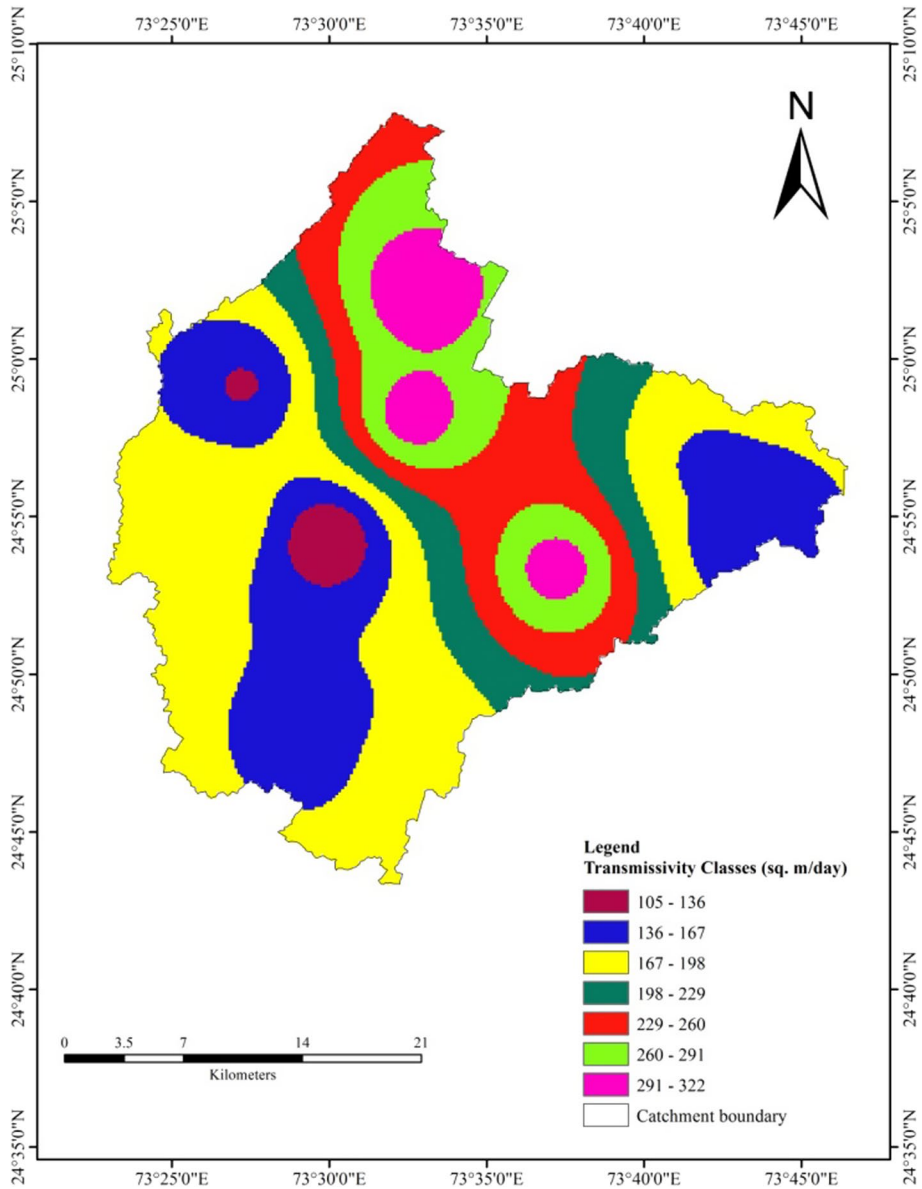
Fig. 11 Transmissivity map

computation of the final normal weights of all thematic layers and their features, thematic layers were transformed to a raster format and then concatenated together with the help of the raster calculator in ArcGIS environment. After computing the final weights of all the TLs and their related features, thematic layers were transformed to a raster format and then concatenated together with the help of the raster calculator in ArcGIS software to produce GWPz. The total score calculated for the GWPz (Fig. 15a, b) was categorized into four
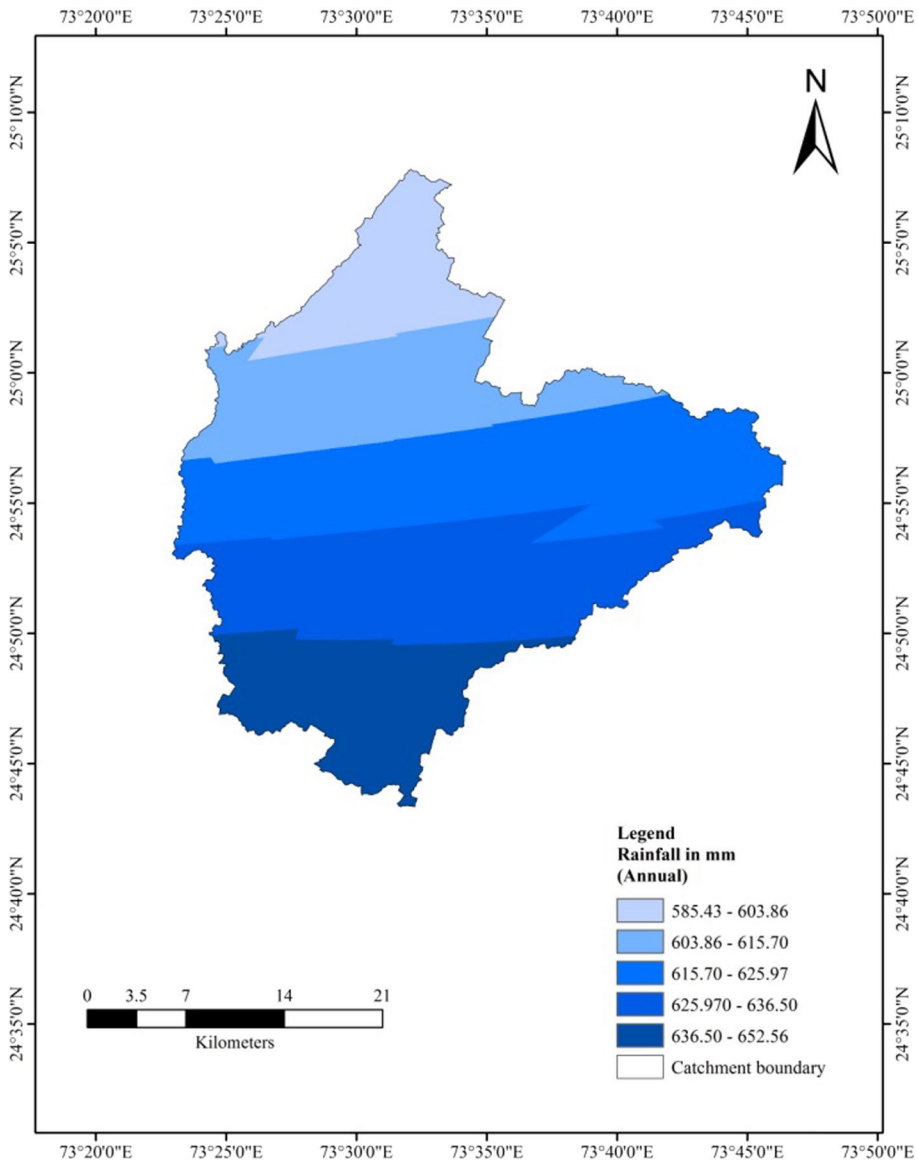
Fig. 12 Thematic map of rainfall distribution

zones: 'G,' 'M,' 'P' and 'VP' groundwater potential. The research findings revealed that the area covered by 'good' GWPz is about 21.23%. The southeast portion and some small patches of western side of the study area have 'M' groundwater potential, and it occupies 53.18% area. About 23.76% area shows poor GWPz. 1.82% of the study region has very poor groundwater potential. As seen from Fig. 15a, the poor and very poor GWPz occur in the steep slope, high drainage density and reserved forests. The findings from this study are comparable to the findings of other groundwater potential studies in many regions globally
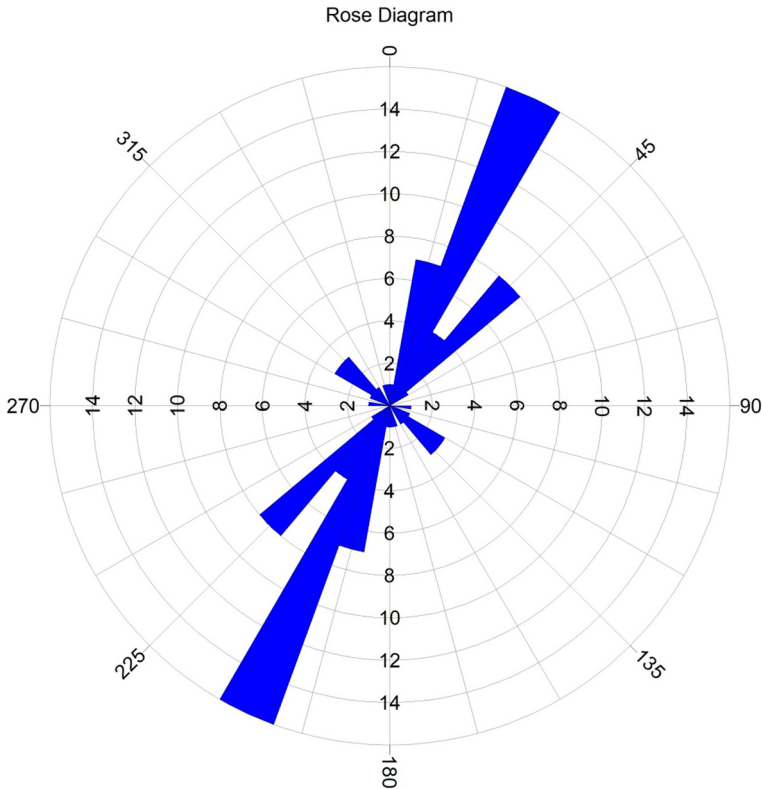
Rose Diagram

Fig. 13 Rose diagram of lineaments of the study area

(Ahmed et al., 2021; Akbari et al., 2021; Al-Manmi et al., 2021; Arulbalaji et al., 2019; Castillo et al., 2022; Hagos & Andualem, 2021; Owolabi et al., 2020). Jhariya et al. (2021) used the AHP method to assess GWPz in the Raipur city by using nine thematic layers and revealed that the medium–high class has maximum percentage (33.92%) of area of potential zones. Pande et al. (2019) applied an integrated approach for the delineation of GWPz of Devdari watershed of Maharashtra. The study results revealed that the good zones are in 9.51 km^2 and very good 14.665 km^2 area of the total area of the watershed. Raju et al. (2019) integrated RS, GIS and multi-influence factor (MIF) techniques for predicting GWPz in Mandavi River basin. Result of the study showed the good class of potential zone having area of 21% out of total study area. Rane and Jayaraj (2021) studied the multi-influence factor (MIF), weight of evidence (WofE) and frequency ratio (FR) technique to evaluate groundwater potential zones in the Kadva river, a tributary of Godavari River. The results of validation showed that the groundwater potential delineated using MIF technique has a prediction accuracy of 81.94%, followed by WofE technique (76.19%) and FR techniques (71.43%). Priya et al. (2022) employed eight thematic layers for the delineation of groundwater potential zones using AHP technique in the Mymensingh district. The results showed that 11.51% of the study area is under a very high groundwater potential zone. Pandey et al. (2022) conducted a study in the district Mahoba, Uttar Pradesh, India, for the GWPz identification by using AHP and Dempster–Shafer model. Results revealed that the
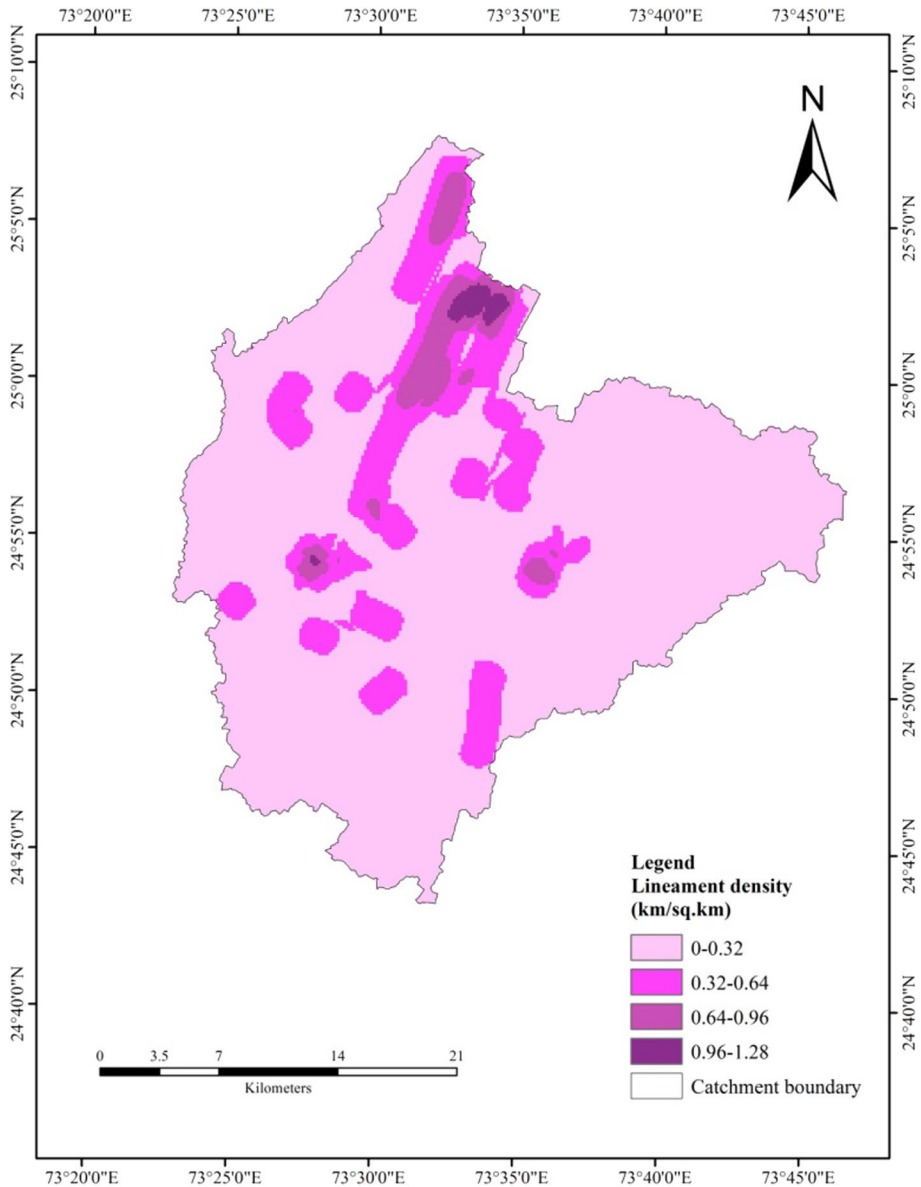
Fig. 14 Lineament density map of the research area

northwest side of the study area is characterized with very high potential zones. The findings of this study were comparable to those of other studies conducted in various parts of India. As a result, the findings of this study can be used as a guideline for further investigation of groundwater development projects.

Validation of the delineated GWPz by using AHP method has been performed by using the existing 16 well discharge data (Table 7) of the study area (Fig. 15a) and ROC method.
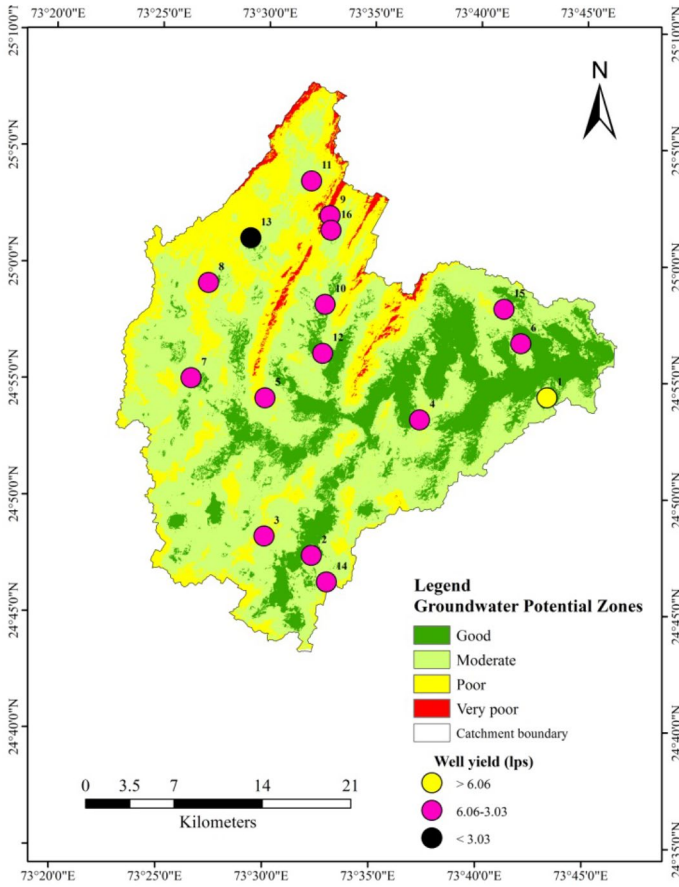
(a)
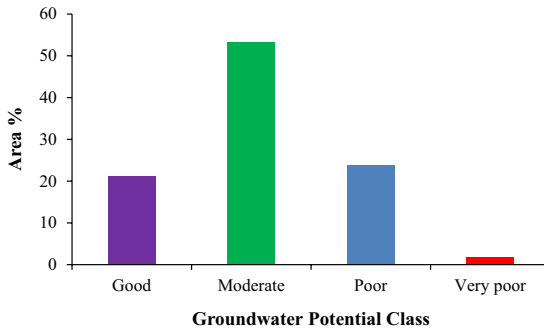
(b)

Fig. 15 a Groundwater potential zones and well locations of the research area **b** groundwater potential classes

The discharge data of the wells are grouped into high (> 6.06 lps), medium (3.03–6.06 lps) and low yield (< 3.03 lps). Table 7 shows the actual yield data obtained from the pumping test, as well as the acceptance/rejection of values that represent open well deviation yield data between expected/real in the form of the agreement. The accuracy prediction [(13/16)×100=81.25%] shows that the selected technique used in this study is considerably reliable and accurate. Such a validation method was used by many researchers like, Pande et al. (2019), Gebru et al. (2020), Al-Manmi et al. (2021), Hibi et al. (2021), Jhariya et al. (2021) and Priya et al. (2022). In the study, there are 16 samples; the greater the AUC, the more accurately the model predicts 0 classes as 0 and 1 classes as 1. The ROC plot obtained is depicted in Fig. 16. The area under the ROC curve is found 0.889 (88.9%) at a significance value of < 0.001. As a result, the high value of AUC validates the suggested approach's efficacy in predicting low and middle/high yield locations. Jhariya et al. (2021) found the ROC curve (AUC) 0.857 (85.7%). Melese and Belay (2022) found the AUC=82.9% which shows the very good accuracy of the model. Similarly, Castillo et al. (2022), Kaewdum and Chotpantarat (2021) and Pandey et al. (2022) also used the ROC method for the validation.

Trabelsi et al. (2022) used AHP technique for the delineation of groundwater potential zones in the Sfax Basin in eastern part of Tunisia. They used wells discharge data and curve trend of sensitivity classes theory for the validation of the applied technique in GWPz. The results showed that the excellent and good potentiality classes have high to very high productivity in the majority of cases.

Table 7 Accuracy assessment of calculated groundwater potential map

Well No.	Longitude	Latitude	Discharge (liter per second)	Actual yield description	Expected yield description from GWPz map	Agreement between actual and expected yields description
1	73.720214	24.905745	9.10	High	High to very high	Agree
2	73.536770	24.791525	5.20	Medium	Medium to high	Agree
3	73.499474	24.804934	5.00	Medium	Medium to high	Disagree
4	73.620434	24.889082	5.73	Medium	Medium to high	Agree
5	73.499109	24.903736	5.73	Medium	Medium to high	Agree
6	73.699274	24.944290	5.67	Medium	Medium to high	Disagree
7	73.440919	24.917505	3.47	Medium	Medium to high	Agree
8	73.453807	24.985906	4.80	Medium	Medium to high	Agree
9	73.548654	25.034824	5.07	Medium	Medium to high	Disagree
10	73.545467	24.971084	5.66	Medium	Medium to high	Agree
11	73.533790	25.059474	4.23	Medium	Medium to high	Agree
12	73.543940	24.936048	5.73	Medium	Medium to high	Agree
13	73.486654	25.018237	3.00	Low	Very low to low	Agree
14	73.548797	24.772500	5.20	Medium	Medium to high	Agree
15	73.685797	24.968900	6.00	Medium	Medium to high	Agree
16	73.549500	25.024200	3.20	Medium	Medium to high	Agree

Fig. 16 ROC curve of the validate result
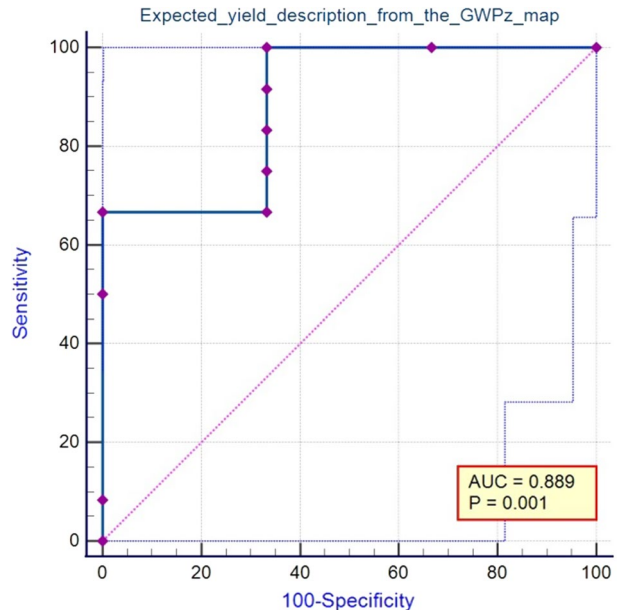
4 Conclusions

The demand for fresh water is a serious concern, so delineating new GWPz cost-effectively is essential to meet freshwater demands. Many scientists have investigated various techniques for evaluating and forecasting the distribution of groundwater for land use planning and water resource management. The majority of agricultural fields rely on groundwater for irrigation. The study region used an integrated view combining geospatial tools and the AHP method to delineate the GWPz. The conclusive groundwater potential map was divided into 4 classes: 'G,' 'M,' 'P' and 'VP.' Results revealed that 21.23% out of the total research area comes under good GWPz, 53.19% of the area under the moderate zone, 23.77% area shows poor GWPz and 1.82% area shows very poor groundwater potential. According to the current study, the research area should focus on groundwater management and development activities. The overall findings indicated that geospatial technologies like RS, GIS and the AHP method have the potential to give a good platform for examining GWPz in hard rock regions and developing appropriate groundwater exploitation plans for many objectives. The integrated map may benefit various developmental activities, including ensuring sustainable groundwater development in the research region and prioritizing locations for water conservation schemes and programs.

Authors' contributions Conceptualization, original draft preparation and editing were performed by Dimple, PKS; methodology, investigation, editing carried out by Dimple, PKS, MK, KKY, SRB; all authors have read and agreed to the published version of the manuscript.

Declarations

Conflict of interest The authors of this article declare that they have no conflict of interests.

References

Abe, M. W., & Ersado, A. E. (2022). Assessment of ground water potential zone based on multi-criteria decision making model and geospatial techniques: The case of Lemo Woreda and Hossana town, Hadiya Zone Southern Nation Nationalities. *Research Square*. https://doi.org/10.2203/rs.3.rs-1717795/v1

Acharya, T. (2017). Delineation of potential groundwater recharge zones in the coastal area of north-eastern India using geoinformatics. *Sustainable Water Resources Management*. https://doi.org/10.1007/s40899-017-0206-4

Adimalla, N., & Venkatayogi, S. (2018). Geochemical characterization and evaluation of groundwater suitability for domestic and agricultural utility in the semi-arid region of Basara, Telangana state South India. *Applied Water Science, 8*, 44.

Ahmed, A., El Ammawy, M., Hewaidy, A. G., Moussa, B., & Hafz, N. A. (2019). Mapping of lineaments for groundwater assessment in the Desert Fringes East El-Minia, Eastern Desert Egypt. *Environmental Monitoring and Assessment, 191*, 1–22.

Ahmed, A., Alrajhi, A., & Alquwaizany, A. S. (2021). Identification of groundwater potential recharge zones in flinders ranges, South Australia using remote sensing, GIS, and MIF techniques. *Water, 13*, 2571. https://doi.org/10.3390/w13182571

Akbari, M., Meshram, S. G., Krishna, R. S., Pradhan, B., Shadeed, S., Khedher, K. M., Sepehri, M., Ildoromi, A. R., Alimerzaei, F., & Darabi, F. (2021). Identification of the groundwater potential recharge zones using MCDM models: Full consistency method (FUCOM), Best worst method (BWM) and Analytic hierarchy process (AHP). *Water Resources Management, 35*, 4727–4745. https://doi.org/10.1007/s11269-021-02924-1

Al-Manmi, D. A. M., Mohammed, S. H., & Szűcs, P. (2021). Integrated remote sensing and GIS techniques to delineate groundwater potential area of Chamchamal basin, Sulaymaniyah NE Iraq. *Kuwait Journal of Science, 48*(3), 1–16.

Anand, B., Karunanidhi, D., & Subramani, T. (2021). Promoting artificial recharge to enhance groundwater potential in the lower Bhavani River basin of South India using geospatial techniques. *Environmental Science and Pollution Research, 28*, 18437–18456. https://doi.org/10.1007/s11356-020-09019-1

Arabameri, A., Roy, J., Saha, S., Blaschke, T., Ghorbanzadeh, O., & Tien Bui, D. (2019). Application of probabilistic and machine learning models for groundwater potentiality mapping in Damghan Sedimentary Plain Iran. *Remote Sensing, 11*(24), 3015.

Arulbalaji, P., Padmalal, D., & Sreelash, K. (2019). GIS and AHP techniques based delineation of groundwater potential zones: A case study from southern Western Ghats India. *Scientific Reports, 9*(1), 2082. https://doi.org/10.1038/s41598-019-38567-x

Bagyaraj, M., Ramkumar, T., Venkatramanan, S., & Gurugnanam, B. (2013). Application of remote sensing and GIS analysis for identifying groundwater potential zone in parts of Kodaikanal Taluk South India. *Frontiers of Earth Science, 7*(1), 65–75. https://doi.org/10.1007/s11707-012-03476

Bera, A., Mukhopadhyay, B. P., & Barua, S. (2020). Delineation of groundwater potential zones in Karha river basin, Maharashtra, India, using AHP and geospatial techniques. *Arabian Journal of Geosciences, 13*, 693. https://doi.org/10.1007/s12517-020-05702-2

Bhattacharya, S., Das, S., Das, S., Kalashetty, M., & Warghat, S. R. (2020). An integrated approach for mapping groundwater potential applying geospatial and MIF techniques in the semiarid region. *Environment, Development and Sustainability*. https://doi.org/10.1007/s10668-020-00593-5

Burek, P., Satoh, Y., Fischer, G., Kahil, M.T., Scherzer, A., & Tramberend, S. (2016). Water futures and solution: Fast track initiative (Final Report). Laxenburg, Austria: IIASA Working Paper, International Institute for Applied Systems Analysis (IIASA).

Castillo, J. L. U., Cruz, D. A. M., Leal, J. A. R., Vargas, J. T., Tapia, S. A. R., & Celestino, A. E. M. (2022). Delineation of groundwater potential zones (GWPZs) in a semi-arid basin through remote sensing, GIS, and AHP approaches. *Water, 14*, 2138. https://doi.org/10.3390/w14132138

Central Groundwater Board (2017). Mahoba District Report. http://cgwb.gov.in/AQM/NAQUIM_REPORT/UP/Mahoba%20NAQUIM%20Report.Pdf

CGWB (2014). Groundwater yearbook, 2014. Central Ground Water Board (CGWB), Ministry of Water Resources, Government of India, pp. 76.

CGWB (2013). Central Ground Water Board. Ground Water Information Rajsamand district Rajasthan, Government of India Ministry of Water Resources, Western Region Jaipur.

Chaudhry, A. K., Kumar, K., & Alam, M. A. (2019). Mapping of groundwater potential zones using the fuzzy analytic hierarchy process and geospatial technique. *Geocarto International, 36*, 2323–2344.

Das, S., & Pardeshi, S. D. (2018). Integration of different influencing factors in GIS to delineate groundwater potential areas using IF and FR techniques: A study of Pravara basin, Maharashtra India. *Applied Water Science, 8*, 1–16.

Das, S., Gupta, A., & Ghosh, S. (2017). Exploring groundwater potential zones using MIF technique in semi-arid region: A case study of Hingoli district Maharashtra. *Spatial Information Research, 25*(6), 749–756. https://doi.org/10.1007/s41324-017-0144-0

Dimple, Rajput, J., Al-Ansari, N., & Elbetagi, A. (2022). Predicting irrigation water quality indices based on data-driven algorithms: Case study in semiarid environment. *Journal of Chemistry.* https://doi.org/10.1155/2022/4488446. Article ID 4488446.

Doke, A. B., Zolekar, R. B., Patel, H., & Das, S. (2021). Geospatial mapping of groundwater potential zones using multi-criteria decision-making AHP approach in a hardrock basaltic terrain in India. *Ecological Indicators, 127*, 107685. https://doi.org/10.1016/j.ecolind.2021.107685

Edmunds, W. M., Shand, P., Hart, P., & Ward, R. S. (2003). The natural (baseline) quality of groundwater: A UK pilot study. *Science of the Total Environment, 310*(1–3), 25–35.

Fagbohun, B. J. (2018). Integrating GIS and multi-influencing factor technique for delineation of potential groundwater recharge zones in parts of Ilesha schist belt, southwestern Nigeria. *Environment and Earth Science, 77*, 1–18.

Gebru, H., Gebreyohannes, T., & Hagos, E. (2020). Identification of groundwater potential zones using analytical hierarchy process (AHP) and GIS-remote sensing integration, the case of Golina River Basin, Northern Ethiopia. *International Journal of Advanced Remote Sensing and GIS, 9*(1), 3289–3311. https://doi.org/10.23953/cloud.ijarsg.460. ISSN 2320–0243.

Ghosh, P. K., Bandyopadhyay, S., & Jana, N. C. (2016). Mapping of groundwater potential zones in hard rock terrain using geoinformatics: A case of Kumari watershed in western part of West Bengal. *Modeling Earth Systems and Environment, 2*(1), 1. https://doi.org/10.1007/s40808-015-0044-z

GWDR (2013). Ground Water Department Rajasthan. Hydrogeological atlas of Rajasthan Rasamand district.

Hagos, Y. G., & Andualem, T. G. (2021). Geospatial and multi-criteria decision approach of groundwater potential zone identification in Cuma sub-basin Southern Ethiopia. *Heliyon, 7*, e07963. https://doi.org/10.1016/j.heliyon.2021.e07963

Harinarayana, P., Gopalakrishna, G. S., & Balasubramanaian, A. (2000). Remote sensing data for groundwater development and management in Keralapura watersheds of Cauvery basin, Karnataka India. *Indian Mineral, 34*(2), 11–17.

Hibi, A., Gouaidia, L., & Guefaifia, O. (2021). Investigation of groundwater potential using remote sensing and hydro-geophysical techniques: A case study of the Telidjene Basin (Eastern Algeria). *Environmental Research, Engineering and Management, 77*(4), 99–121.

Jasrotia, A. S., Kumar, A., & Singh, R. (2016). Integrated remote sensing and GIS approach for delineation of groundwater potential zones using aquifer parameters in Devak and Rui watershed of Jammu and Kashmir India. *Arabian Journal of Geosciences, 9*(4), 1–15. https://doi.org/10.1007/s12517-016-2326-9

Jesiya, N. P., & Gopinath, G. A. (2020). Fuzzy based MCDM–GIS framework to evaluate groundwater potential index for sustainable groundwater management-A case study in an urban-periurban ensemble, southern India. *Groundwater for Sustainable Development, 11*, 100466.

Jhariya, D. C., Khan, R., Mondal, K. C., Kumar, T., Indhulekha, K., & Singh, V. K. (2021). Assessment of groundwater potential zone using GIS-based multi-influencing factor (MIF), multi-criteria decision analysis (MCDA) and electrical resistivity survey techniques in Raipur city, Chhattisgarh, India. *Aqua-Water Infrastructure, Ecosystem and Society, 70*, 3.

Kaewdum, N., & Chotpantarat, S. (2021). Mapping potential zones for groundwater recharge using a GIS technique in the lower Khwae Hanuman Sub-Basin Area, Prachin Buri Province, Thailand. *Frontiers in Earth Science, 9*, 717313.

Kumar, A., & Krishna, A. P. (2018). Assessment of groundwater potential zones in coal mining impacted hard-rock terrain of India by integrating geospatial and analytic hierarchy process (AHP) approach. *Geocarto International, 33*(2), 105–129. https://doi.org/10.1080/10106049.2016.1232314

Kumar, P., Herath, S., Avtar, R., & Takeuchi, K. (2016). Mapping of groundwater potential zones in Killinochi area, Sri Lanka, using GIS and remote sensing techniques. *Sustainable Water Resources Management, 2*(4), 419–430. https://doi.org/10.1007/s40899-016-0072-5

Lentswe, G. B., & Molwalefhe, L. (2020). Delineation of potential groundwater recharge zones using analytic hierarchy process-guided GIS in the semi-arid Motloutse watershed, eastern Botswana. *Journal of Hydrology: Regional Studies, 28*, 100674.

Machiwal, D., & Jha, M. K. (2014). Characterizing rainfall-groundwater dynamics in a hard-rock aquifer system using time series, geographic information systemand geostaticalmodelling. *Hydrological Processes, 28*, 2824–2843.

Machiwal, D., & Singh, P. K. (2015). Comparing GIS-based multi-criteria decision-making and Boolean logic modelling approaches for delineating groundwater recharge zones. *Arabian Journal of Geosciences, 8*(12), 10675–10691. https://doi.org/10.1007/s12517015-2002-5

Machiwal, D., Jha, M. K., & Mal, B. C. (2011). Assessment of groundwater potential in a semiarid region of India using remote sensing, GIS and MCDM techniques. *Water Resources Management, 25*(5), 1359–1386. https://doi.org/10.1007/s11269-010-9749-y

Machiwal, D., Singh, P. K., & Yadav, K. K. (2017). Estimating aquifer properties and distributed groundwater recharge in a hard-rock catchment of Udaipur India. *Applied Water Science, 7*, 3157–3172. https://doi.org/10.1007/s13201-016-0462-8

Makonyo, M., & Msabi, M. M. (2021). Identification of groundwater potential recharge zones using GIS-based multi-criteria decision analysis: A case study of semi-arid midlands Manyara fractured aquifer, North-Eastern Tanzania. *Remote Sensing Applications: Society and Environment, 23*, 100544.

Manap, M. A., Nampak, H., Pradhan, B., Lee, S., Sulaiman, W. N. A., & Ramli, M. F. (2014). Application of probabilistic-based frequency ratio model in groundwater potential mapping using remote sensing data and GIS. *Arabian Journal of Geosciences, 7*(2), 711–724. https://doi.org/10.1007/s12517-012-0795-z

Melese, T., & Belay, T. (2022). Groundwater potential zone mapping using analytical hierarchy process and GIS in Muga Watershed, Abay Basin Ethiopia. *Global Challenges, 6*, 2100068.

Mir, S., Bhat, M. S., Rather, G. M., & Mattoo, D. (2021). Groundwater potential zonation using integration of remote sensing and AHP/ANP approach in North Kashmir, Western Himalaya India. *Remote Sensing of Land, 5*, 41–58.

Mukherjee, P., Singh, C. K., & Mukherjee, S. (2012). Delineation of groundwater potential zones in arid region of India—A remote sensing and GIS approach. *Water Resources Management, 26*(9), 2643–2672. https://doi.org/10.1007/s11269-012-0038-9

Murmu, P., Kumara, M., Lala, D., Sonkerb, I., & Singh, S. K. (2019). Delineation of groundwater potential zones using geospatial techniques and analytical hierarchy process in Dumka district, Jharkhand India. *Groundwater for Sustainable Development, 9*, 100239. https://doi.org/10.1016/j.gsd.2019.100239

Nag, S. K., & Ghosh, P. (2013). Delineation of groundwater potential zone in Chhatna Block. Bankura District, West Bengal, India using remote sensing and GIS techniques. *Environment and Earth Science, 70*, 2115–2127.

Owolabi, S. T., Madi, K., Kalumba, A. M., & Orimoloye, I. R. (2020). A groundwater potential zone mapping approach for semi-arid environments using remote sensing (RS), geographic information system (GIS), and analytical hierarchical process (AHP) techniques: A case study of Buffalo catchment, Eastern Cape South Africa. *Arabian Journal of Geosciences, 13*, 1184. https://doi.org/10.1007/s12517-020-06166-0

Pande, C. B., Moharir, K. N., Singh, S. K., & Varade, A. M. (2019). An integrated approach to delineate the groundwater potential zones in Devdari watershed area of Akola district, Maharashtra Central India. *Environment, Development and Sustainability.* https://doi.org/10.1007/s10668-019-00409-1

Pandey, H. K., Singh, V. K., & Singh, S. K. (2022). Multi-criteria decision making and Dempster-Shafer model–based delineation of groundwater prospect zones from a semi-arid environment. *Environmental Science and Pollution Research, 29*, 47740–47758. https://doi.org/10.1007/s11356-022-19211-0

Priya, U., Iqbal, M. A., Salam, M. A., Nur-E-Alam, Md., Uddin, M. F., Islam, T., Abu Reza, Md., Sarkar, S. K., Imran, S. I., & Rak, AEh. (2022). Sustainable groundwater potential zoning with integrating GIS, remote sensing, and AHP model: A case from north-central Bangladesh. *Sustainability, 14*, 5640. https://doi.org/10.3390/su14095640

Rahmati, O., Nazari Samani, A., Mahdavi, M., Pourghasemi, H. R., & Zeinivand, H. (2015). Groundwater potential mapping at Kurdistan region of Iran using analytic hierarchy process and GIS. *Arabian Journal of Geosciences, 8*(9), 7059–7071. https://doi.org/10.1007/s12517-014-1668-4

Rajasekhar, M., Gadhiraju, S. R., Kadam, A., & Bhagat, V. (2020). Identification of groundwater recharge-based potential rainwater harvesting sites for sustainable development of a semiarid region of southern India using geospatial, AHP, and SCS-CN approach. *Arabian Journal of Geosciences, 13*(2), 24. https://doi.org/10.1007/s12517-019-4996-6

Raju, R. S., Raju, G. S., & Rajasekhar, M. (2019). Identification of groundwater potential zones in Mandavi River basin, Andhra Pradesh, India using remote sensing, GIS and MIF techniques. *HydroResearch, 2*, 1–11. https://doi.org/10.1016/j.hydres.2019.09.001

Rane, N. L., & Jayaraj, G. K. (2021). Comparison of multi-influence factor, weight of evidence and frequency ratio techniques to evaluate groundwater potential zones of basaltic aquifer systems. *Environment, Development and Sustainability.* https://doi.org/10.1007/s10668-021-01535-5

Saaty, T. L. (1990). How to make a decision: The analytic hierarchy process. *European Journal of Operational Research, 48*(1), 9–26. https://doi.org/10.1016/0377-2217(90)90057-I

Saaty, T. L. (1980). The analytic hierarchy process: Planning, priority setting, resource allocation.

Saeid, S., Chizari, M., Sadighi, H., & Bijani, M. (2018). Assessment of agricultural groundwater users in Iran: A cultural environmental bias. *Hydrogeology Journal, 26*, 285–295. https://doi.org/10.1007/s10040-017-1634-9

Sahu, U., Wagh, V., Mukate, S., Kadam, A., & Patil, S. (2022). Applications of geospatial analysis and analytical hierarchy process to identify the groundwater recharge potential zones and suitable recharge structures in the Ajani-Jhiri watershed of north Maharashtra India. *Groundwater for Sustainable Development, 17*, 100733.

Sajil-Kumar, P. J., Elango, L., & Schneider, M. (2022). GIS and AHP based groundwater potential zones delineation in Chennai River Basin (CRB) India. *Sustainability, 14*, 1830.

Shaban, A., Khawlie, M., & Abdallah, C. (2006). Use of remote sensing and GIS to determine recharge potential zones: The case of occidental Lebanon. *Hydrogeology Journal, 14*(4), 433–443. https://doi.org/10.1007/s10040-005-0437-6

Shekhar, S., & Pandey, A. C. (2015). Delineation of groundwater potential zone in hard rock terrain of India using remote sensing, geographical information system (GIS) and analytic hierarchy process (AHP) techniques. *Geocarto International, 30*(4), 402–421. https://doi.org/10.1080/10106049.2014.894584

Singh, L. K., Jha, M. K., Chowdary, V. M. (2018). Assessing the accuracy of GIS-based Multi-Criteria Decision Analysis approaches for mapping groundwater potential. Ecological Indicator *91*, 24–37.

Singh, C. K., Shashtri, S., Singh, A., & Mukherjee, S. (2011). Quantitative modeling of groundwater in Satluj river basin of Rupnagar district of Punjab using remote sensing and geographic information system. *Environment and Earth Science, 62*(4), 871–881. https://doi.org/10.1007/s12665-010-0574-7

Singh, P., Hasnat, M., Rao, M. N., & Singh, P. (2021). Fuzzy analytical hierarchy process based GIS modelling for groundwater prospective zones in Prayagraj India. *Groundwater for Sustainable Development, 12*, 100530.

Singha, S. S., Pasupuleti, S., Singha, S., Singh, R., & Venkatesh, A. S. (2019). Analytic network process based approach for delineation of groundwater potential zones in Korba district, Central India using remote sensing and GIS. *Geocarto International, 36*, 1489–1511.

Sresto, M. A., Siddika, S., Haque, M. N., & Saroar, M. (2021). Application of fuzzy analytic hierarchy process and geospatial technology to identify groundwater potential zones in northwest region of Bangladesh. *Environmental Challenges, 5*, 100214.

Suliman, M., Samiullah, K., & Ali, M. (2022). Identification of potential groundwater recharge sitein a semi-arid region of Pakistan using Saaty's analytical hierarchical process (Ahp). *Geomatics and Environmental Engineering, 16*, 53–70.

Trabelsi, N., Hentati, I., Triki, I., Zairi, M., & Banton, O. (2022). A GIS-Agriflux modeling and AHP techniques for groundwater potential zones mapping. *Journal of Geographic Information System, 14*, 113–133.

UNESCO (2018). Nature-based solutions for water. The United Nations World Water Development Report (WWDR), World Water Assessment Program, UNESCO, Paris, France.

Vishwakarma, A., Goswami, A., & Pradhan, B. (2021). Prioritization of sites for managed aquifer recharge in a semi-arid environment in western India using GIS-based multi-criteria evaluation strategy. *Groundwater for Sustainable Development, 12*, 100501.

World Bank (2010). Deep wells and prudence: Towards pragmatic action for addressing groundwater over-exploitation in India. World Bank Report No. 51676, Washington, DC: World Bank.

Yeh, H. F., Lee, C. H., Hsu, K. C., & Chang, P. H. (2009). GIS for the assessment of the groundwater recharge potential zone. *Environmental Geology, 58*, 185–195.

Authors and Affiliations

Dimple[1] · Pradeep Kumar Singh[1] · Mahesh Kothari[1] · Kamal Kishore Yadav[2] · Sita Ram Bhakar[1]

Pradeep Kumar Singh
pksingh35@yahoo.com

Mahesh Kothari
drmkothari@hotmail.com

Kamal Kishore Yadav
kkyadavctae@gmail.com

Sita Ram Bhakar
srbhakar@gmail.com

[1] Department of Soil and Water Engineering, College of Technology and Engineering, MPUAT, Udaipur, Rajasthan 313001, India

[2] Department of Agricultural Chemistry and Soil Science, Rajasthan College of Agriculture, MPUAT, Udaipur, Rajasthan 313001, India